

# Field Testing of an Ultra-High Performance Concrete Overlay

PUBLICATION NO. FHWA-HRT-17-096

SEPTEMBER 2017



U.S. Department of Transportation  
**Federal Highway Administration**

Research, Development, and Technology  
Turner-Fairbank Highway Research Center  
6300 Georgetown Pike  
McLean, VA 22101-2296

## FOREWORD

Ultra-high performance concrete (UHPC) is an advanced construction material that can positively influence the future of the highway infrastructure. Since 2001, the Federal Highway Administration (FHWA) has been at the forefront of developing UHPC-based solutions for pressing challenges. One problem facing many bridge owners is the urgent need for effective and durable rehabilitation solutions for deteriorated highway bridge decks. An emerging solution to this problem is thin, bonded UHPC overlays which have durability and mechanical properties that exceed those of conventional overlay solutions. This report documents the first deployment of a UHPC overlay in the United States and the field testing used to validate its installation and initial performance. The information presented provides foundational knowledge to bridge owners and designer consultants interested in using this innovative solution for preserving our Nation's highway bridges.

Cheryl Allen Richter, P.E., Ph.D.  
Director, Office of Infrastructure  
Research and Development

### Notice

This document is disseminated under the sponsorship of the U.S. Department of Transportation in the interest of information exchange. The U.S. Government assumes no liability for the use of the information contained in this document.

The U.S. Government does not endorse products or manufacturers. Trademarks or manufacturers' names appear in this report only because they are considered essential to the objective of the document.

### Quality Assurance Statement

The Federal Highway Administration (FHWA) provides high-quality information to serve Government, industry, and the public in a manner that promotes public understanding. Standards and policies are used to ensure and maximize the quality, objectivity, utility, and integrity of its information. FHWA periodically reviews quality issues and adjusts its programs and processes to ensure continuous quality improvement

## TECHNICAL REPORT DOCUMENTATION PAGE

1. Report No. FHWA-HRT-17-096	2. Government Accession No.	3. Recipient's Catalog No.	
4. Title and Subtitle Field Testing of an Ultra-High Performance Concrete Overlay		5. Report Date October 2017	
		6. Performing Organization Code:	
7. Author(s) Zachary B. Haber, Jose F. Munoz, and Benjamin A. Graybeal		8. Performing Organization Report No.	
9. Performing Organization Name and Address Office of Infrastructure Research & Development Federal Highway Administration 6300 Georgetown Pike McLean, VA 22101-2296		10. Work Unit No.	
		11. Contract or Grant No.	
12. Sponsoring Agency Name and Address Office of Infrastructure Research & Development Federal Highway Administration 6300 Georgetown Pike McLean, VA 22101-2296		13. Type of Report and Period Covered Final Report: April 2016–May 2017	
		14. Sponsoring Agency Code HRDI-40	
15. Supplementary Notes The document content was prepared by Zachary Haber of Genex Systems, LLC, under laboratory support contract DTFH61-16-D-00033, and Jose F. Munoz of SES Group and Associates, LLC under laboratory support contract DTFH61-13-D-00007.			
16. Abstract Bridge decks are commonly rehabilitated using overlays depending on the cause of deck deterioration, available budget, and desired service life of the rehabilitated structure. One emerging solution for bridge deck rehabilitation is thin, bonded ultra-high performance concrete (UHPC) overlays. As an overlay material, UHPC can provide both structural strengthening and protection from ingress of contaminants using a 1-in (25 mm) to 2-in (51 mm) layer of material. The first U.S. deployment of UHPC as a bridge deck overlay was completed in May 2016 on a reinforced concrete slab bridge located in Brandon. A few months after installing the UHPC overlay, a field inspection of the bridge identified some locations along the deck where delamination may have occurred. To address this concern, a field study was conducted in November 2016 to evaluate the bond between the UHPC overlay and the substrate concrete bridge deck. Researchers from the Federal Highway Administration's (FHWA) Turner-Fairbank Highway Research Center (TFHRC) synthesized photographic evidence, conducted a field inspection of the bridge deck surface using a chain drag, and conducted physical testing of the UHPC-concrete interface bond using the direct tension bond pull-off test. Tested samples were taken back to TFHRC and the UHPC-concrete interface subsequently analyzed using scanning electron microscopy (SEM). The pull-off test data indicated that the UHPC overlay and the existing concrete bridge deck was intact, which was confirmed by SEM analysis.			
17. Key Words Ultra-high performance concrete, overlay, delamination, bond, scarification, hydrodemolition		18. Distribution Statement No Restrictions. This document is available through the National Technical Information Service, Springfield, VA 22161. <a href="http://www.ntis.gov">http://www.ntis.gov</a>	
19. Security Classif. (of this report) Unclassified	20. Security Classif. (of this page) Unclassified	21. No. of Pages 57	22. Price N/A

# SI\* (MODERN METRIC) CONVERSION FACTORS

## APPROXIMATE CONVERSIONS TO SI UNITS

Symbol	When You Know	Multiply By	To Find	Symbol
<b>LENGTH</b>				
in	inches	25.4	millimeters	mm
ft	feet	0.305	meters	m
yd	yards	0.914	meters	m
mi	miles	1.61	kilometers	km
<b>AREA</b>				
in <sup>2</sup>	square inches	645.2	square millimeters	mm <sup>2</sup>
ft <sup>2</sup>	square feet	0.093	square meters	m <sup>2</sup>
yd <sup>2</sup>	square yard	0.836	square meters	m <sup>2</sup>
ac	acres	0.405	hectares	ha
mi <sup>2</sup>	square miles	2.59	square kilometers	km <sup>2</sup>
<b>VOLUME</b>				
fl oz	fluid ounces	29.57	milliliters	mL
gal	gallons	3.785	liters	L
ft <sup>3</sup>	cubic feet	0.028	cubic meters	m <sup>3</sup>
yd <sup>3</sup>	cubic yards	0.765	cubic meters	m <sup>3</sup>
NOTE: volumes greater than 1000 L shall be shown in m <sup>3</sup>				
<b>MASS</b>				
oz	ounces	28.35	grams	g
lb	pounds	0.454	kilograms	kg
T	short tons (2000 lb)	0.907	megagrams (or "metric ton")	Mg (or "t")
<b>TEMPERATURE (exact degrees)</b>				
°F	Fahrenheit	5 (F-32)/9 or (F-32)/1.8	Celsius	°C
<b>ILLUMINATION</b>				
fc	foot-candles	10.76	lux	lx
fl	foot-Lamberts	3.426	candela/m <sup>2</sup>	cd/m <sup>2</sup>
<b>FORCE and PRESSURE or STRESS</b>				
lbf	poundforce	4.45	newtons	N
lbf/in <sup>2</sup>	poundforce per square inch	6.89	kilopascals	kPa
<b>APPROXIMATE CONVERSIONS FROM SI UNITS</b>				
Symbol	When You Know	Multiply By	To Find	Symbol
<b>LENGTH</b>				
mm	millimeters	0.039	inches	in
m	meters	3.28	feet	ft
m	meters	1.09	yards	yd
km	kilometers	0.621	miles	mi
<b>AREA</b>				
mm <sup>2</sup>	square millimeters	0.0016	square inches	in <sup>2</sup>
m <sup>2</sup>	square meters	10.764	square feet	ft <sup>2</sup>
m <sup>2</sup>	square meters	1.195	square yards	yd <sup>2</sup>
ha	hectares	2.47	acres	ac
km <sup>2</sup>	square kilometers	0.386	square miles	mi <sup>2</sup>
<b>VOLUME</b>				
mL	milliliters	0.034	fluid ounces	fl oz
L	liters	0.264	gallons	gal
m <sup>3</sup>	cubic meters	35.314	cubic feet	ft <sup>3</sup>
m <sup>3</sup>	cubic meters	1.307	cubic yards	yd <sup>3</sup>
<b>MASS</b>				
g	grams	0.035	ounces	oz
kg	kilograms	2.202	pounds	lb
Mg (or "t")	megagrams (or "metric ton")	1.103	short tons (2000 lb)	T
<b>TEMPERATURE (exact degrees)</b>				
°C	Celsius	1.8C+32	Fahrenheit	°F
<b>ILLUMINATION</b>				
lx	lux	0.0929	foot-candles	fc
cd/m <sup>2</sup>	candela/m <sup>2</sup>	0.2919	foot-Lamberts	fl
<b>FORCE and PRESSURE or STRESS</b>				
N	newtons	0.225	poundforce	lbf
kPa	kilopascals	0.145	poundforce per square inch	lbf/in <sup>2</sup>

\*SI is the symbol for the International System of Units. Appropriate rounding should be made to comply with Section 4 of ASTM E380.  
(Revised March 2003)

## TABLE OF CONTENTS

<b>CHAPTER 1. INTRODUCTION.....</b>	<b>1</b>
<b>INTRODUCTION .....</b>	<b>1</b>
<b>PROBLEM STATEMENT AND OBJECTIVE .....</b>	<b>4</b>
<b>APPROACH.....</b>	<b>5</b>
<b>REPORT OUTLINE .....</b>	<b>5</b>
<b>CHAPTER 2. BACKGROUND AND PREVIOUS RESEARCH.....</b>	<b>7</b>
<b>PROPERTIES OF UHPC-CLASS MATERIALS.....</b>	<b>7</b>
<b>UHPC AS A BRIDGE DECK OVERLAY MATERIAL.....</b>	<b>8</b>
<b>PREVIOUS UHPC OVERLAY RESEARCH AND DEPLOYMENTS.....</b>	<b>13</b>
<b>CHAPTER 3. DETAILS OF THE LAPORTE ROAD BRIDGE.....</b>	<b>19</b>
<b>BRIDGE DESCRIPTION.....</b>	<b>19</b>
<b>OVERLAY DETAILS.....</b>	<b>20</b>
<b>FIELD OBSERVATIONS PRIOR TO OVERLAY INSTALLATION .....</b>	<b>20</b>
<b>OVERLAY INSTALLATION AND FINISHING.....</b>	<b>21</b>
<b>CHAPTER 4. EVALUATION METHODOLOGY .....</b>	<b>25</b>
<b>INTRODUCTION .....</b>	<b>25</b>
<b>INDENTIFICATION OF TEST LOCATIONS.....</b>	<b>25</b>
<b>BOND TESTING .....</b>	<b>28</b>
<b>SCANNING ELECTRON MICROSCOPY .....</b>	<b>31</b>
<b>CHAPTER 5. RESULTS AND DISCUSSION.....</b>	<b>33</b>
<b>TEST LOCATIONS G1 AND G2 .....</b>	<b>33</b>
<b>TEST LOCATION G3 .....</b>	<b>38</b>
<b>TEST LOCATIONS B1 AND B7 .....</b>	<b>41</b>
<b>SUMMARY OF RESULTS .....</b>	<b>44</b>
<b>CHAPTER 6. SUMMARY AND CONCLUSIONS.....</b>	<b>45</b>
<b>REFERENCES.....</b>	<b>46</b>

## LIST OF FIGURES

Figure 1. Pie Chart. Concrete bridge deck condition rating based on 2016 NBI data.....	1
Figure 2. Pie Chart. Anticipated service life of bridge deck overlays as reported by 43 transportation agencies.....	3
Figure 3. Illustration. Existing concrete bridge deck with a UHPC overlay and potential locations of delamination.....	5
Figure 4. Photo. Nonthixotropic formulation .....	10
Figure 5. Photo. Thixotropic formulation.....	10
Figure 6. Graph. Comparison of the direct tension behavior of thixotropic and nonthixotropic UHPC.....	11
Figure 7. Illustration. Direct tension test method for UHPC.....	11
Figure 8. Graph. Comparison of the direct tension bond strength of thixotropic (Thix) and nonthixotropic (Non-Thix) UHPC formulations .....	12
Figure 9. Illustration. ASTM C1583—Direct tension bond pull-off test method .....	12
Figure 10. Photo. Chillon Viaduct: Parallel post-tensioned box girder structures .....	15
Figure 11. Illustration. Chillon Viaduct Details: Typical section of a single post-tensioned box girder .....	16
Figure 12. Photo. Arial view of the Chillon Viaduct UHPC overlay construction project .....	16
Figure 13. Photo. Placement of UHPC in the Chillon Viaduct project .....	17
Figure 14. Photo. Laporte Road bridge.....	19
Figure 15. Illustration. Typical section showing the UHPC overlay looking eastbound .....	20
Figure 16. Photo. Distressed region observed on the westbound lane over the pier 1 prior to installing the UHPC overlay .....	21
Figure 17. Photo. Distressed region observed on the westbound lane near west abutment prior to installing the UHPC overla. ....	21
Figure 18. Photo. Deck surface after scarification.....	22
Figure 19. Photo. Placement of the UHPC overlay on the westbound lane .....	23
Figure 20. Photo. Curing of the overlay on the westbound lane.....	23
Figure 21. Photo. Completed overlay after deck milling looking eastbound .....	24
Figure 22. Illustration. Schematic of observations, inspection findings, and test locations on the western side of the bridge .....	26
Figure 23. Illustration. Schematic of observations, inspection findings, and test locations on the eastern side of the bridge .....	27
Figure 24. Illustration. Direct tension pull-off bond test based on ASTM C1583 .....	29
Figure 25. Photos. Failure modes associated with the direct tension pull-off bond test; photos taken from previous projects.....	29
Figure 26. Photo. In-situ bond testing on the Laporte Road bridge.....	30
Figure 27. Photo. Preparation of the bond test location on the Laporte Road bridge.....	30
Figure 28. Photo. Two test samples after failure in the substrate concrete .....	31
Figure 29. Illustration. Example of segmentation process on Quantitative map with 10- $\mu$ m-wide bands used to study the distribution of porosity, aggregate, and unhydrated cement particles of the UHPC-concrete interface .....	32
Figure 30. Photo. Test disc removed from samples from G1 and G2 locations .....	34
Figure 31. Photos. Specimen G2-9 after testing .....	34
Figure 32. Photo. Core location for specimen G2-9 .....	35

Figure 33. Electron Microscope Image. General map of the UHPC-concrete interface for specimen G2-8 .....	36
Figure 34. Electron Microscope Image. BSE image of a void between the UHPC overlay and the substrate concrete .....	36
Figure 35. Electron Microscope Image. BSE image of poor consolidation or debris accumulation at the interface .....	37
Figure 36. Graph. Overall distribution at the interface as a function of distance from the concrete surface of specimen G2-8 phases .....	38
Figure 37. Photos. Specimen G3-13 after testing .....	39
Figure 38. Photo. Core location for specimen G3-13 .....	39
Figure 39. Electron Microscope Image. General map of the UHPC-concrete interface for specimen G3-14 .....	40
Figure 40. Graph. Overall distribution at the interface as a function of distance from the concrete surface of specimen G3-14 phases .....	41
Figure 41. Photos. Specimen B7-11 after testing .....	42
Figure 42. Photo. Core location for specimen B7-11 .....	42
Figure 43. Electron Microscope Image. General map of the UHPC-concrete interface for specimen B7-12 .....	43
Figure 44. Graph. Overall distribution at the interface as a function of distance from the concrete surface of the specimen B7-12 phases .....	44

## LIST OF TABLES

Table 1. FHWA Condition ratings—1995 .....	2
Table 2. Typical properties of field-cast UHPC .....	8
Table 3. Approximate cost ranges of bridge deck overlay solutions .....	13
Table 4. Summary of findings from the chain drag and test location details .....	28
Table 5. Summary of results from bond testing.....	33

## LIST OF ABBREVIATIONS

AAR	alkali-aggregate reactivity
AASHTO	American Association of State Highway and Transportation Officials
ABC	accelerated bridge construction
ADT	average daily traffic
ASTM	American Society of Testing and Materials
BSE	backscatter electron
CAD	computer-aided drafting
CSH	calcium silicate hydrated
FEA	finite-element analysis
FHWA	Federal Highway Administration
HPC	high-performance concrete
LMC	latex-modified concrete
NBI	National Bridge Inventory
PBE	prefabricated bridge element
RC	reinforced concrete
SCM	supplementary cementitious materials
SEM	scanning electron microscope
TFHRC	Turner-Fairbank Highway Research Center
UHPC	ultra-high performance concrete



## CHAPTER 1. INTRODUCTION

### INTRODUCTION

Maintenance and rehabilitation of highway bridge decks is a continual challenge for bridge owners and transportation agencies throughout the United States. Transportation agencies must extend the service lives of existing bridge decks with limited funds and limited time needed for replacement or major rehabilitation. For context, figure 1 shows a pie chart depicting the bridge deck condition rating from U.S. bridges currently in service; the data shown is based on 2016 National Bridge Inventory (NBI) data.

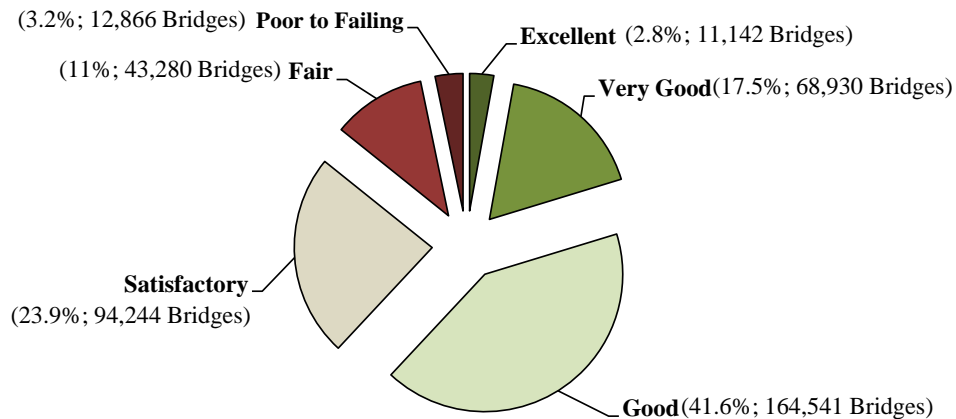


**Figure 1. Pie Chart. Concrete bridge deck condition rating based on 2016 NBI data.**

The data only include highway bridges with reinforced concrete bridge decks, either cast-in-place or precast. Table 1 lists the NBI codes, condition rating, and the associated description for each rating. Approximately 38 percent of these bridges exhibit some level of deck deterioration. This is not to say that this entire group requires remedial action. However, deterioration is progressive and irreversible. Thus, bridges with decks in the satisfactory group will tend to migrate over time to the fair group, and so on. There is currently a need for resilient and durable repair and rehabilitation solutions for these aging reinforced concrete bridge decks.

**Table 1. FHWA Condition ratings—1995.**

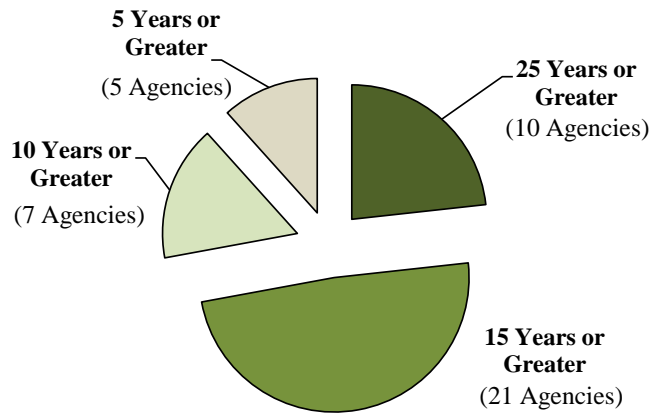
<b>NBI Code</b>	<b>Condition Rating</b>	<b>Description</b>
N	Not Applicable	Pertains to culverts and other structures without decks; e.g., filled arch bridge.
9	Excellent	
8	Very Good	No problems noted
7	Good	Some minor problems
6	Satisfactory	Structural elements show some minor deterioration
5	Fair	All primary structural elements are sound but may have minor section loss, cracking, spalling or scour.
4	Poor	Advanced section loss, deterioration, spalling or scour.
3	Serious	Loss of section, deterioration, spalling or scour have seriously affected primary structural components. Local failures are possible. Fatigue cracks in steel or shear cracks in concrete may be present.
2	Critical	Advanced deterioration of primary structural elements. Fatigue cracks in steel or shear cracks in concrete may be present or scour may have removed substructure support. Unless closely monitored it may be necessary to close the bridge until corrective action is taken.
1	“Imminent” Failure	Major deterioration or section loss present in critical structural components or obvious vertical or horizontal movement affecting structure stability. Bridge is closed to traffic but corrective action may put back in light service.
0	Failed	Out of service—beyond corrective action.

Bridge deck repairs usually have one or a combination of the following objectives:

- Seal existing cracks and areas of spalled concrete.
- Water proof.
- Provide additional protection to corroded or damaged reinforcement.
- Provide a smooth riding surface for increased user comfort.
- Replace deteriorated cover concrete.
- Add material for structural strengthening.

Traditionally, conventional cement- or asphalt-based overlays have been economical and constructible options to achieve these objectives. However, these options also suffer from their own degradation mechanisms. Many transportation agencies fully recognize limited service life extension as noted in the report by Krauss, Lawler, and Steiner (2009).

Figure 2 depicts the anticipated service life of bridge deck overlays as reported by 43 transportation agencies. (Krauss, Lawler, and Steiner 2009) Most agencies feel that overlays will last between 5 and 30 years. However, this data does not reflect actual service life extensions, which may be shorter or longer than anticipated. Nevertheless, there is a need for durable, long-lasting bridge deck overlay solutions to extend the service life of existing bridge structures.



Source: Data from Krauss, Lawler, and Steiner (2009).

**Figure 2. Pie Chart. Anticipated service life of bridge deck overlays as reported by 43 transportation agencies.**

Ultra-high performance concrete is emerging as an innovative solution for a variety of bridge construction and rehabilitation applications, including 100 percent UHPC structural elements, structural patching and repair bridge element, jackets for columns and driven piles, and field-cast connections between prefabricated bridge elements. One emerging application of UHPC in the highway bridge sector is thin, bonded overlays for bridge deck rehabilitation. As an overlay material, UHPC can provide both structural strengthening and protection from chloride penetration and water ingress. This is achieved using a 1-in (25-mm) to 2-in (51-mm) thick layer of UHPC, which minimizes both the required material volume and additional dead load on the bridge structure. Prior to placing the UHPC overlay, a thin layer of poor and/or deteriorated concrete is removed from the existing concrete deck (if needed), and the deck surface is roughened to facilitate good bond between UHPC and existing concrete. Good bond between the UHPC overlay and the existing concrete deck is required to develop composite action between the two materials. The concept and use of UHPC overlays has been researched in Europe and has been deployed on more than 20 bridges. (Brühwiler and Denarié 2013)

## UHPC BACKGROUND

Advances in concrete technology, such as high-strength steel micro-fiber reinforcement, superplasticizers, gradation optimization, and supplementary cementitious materials, began to be packaged together into a new generation of cementitious composite materials in the 1970s and 1980s. In the 1990s, this new class of materials was brought to market and has become known as ultra-high performance concrete (UHPC). Preblended, prepackaged, proprietary formulations of UHPC became commercially available in the United States in the early 2000s, and academic

researchers funded by Federal or State transportation agencies have developed nonproprietary mixes. (Wille and Boisvert-Cotulio 2013; El-Tawil et al. 2016)

UHPC offers a number of advantages over conventional concretes and other cementitious materials, including enhanced material and durability properties, which have gained the attention of the highway bridge design community. Since 2005, over 140 highway bridges have been constructed using UHPC in the United States and Canada combined. Those deployments used UHPC in a variety of bridge construction and rehabilitation applications, including prefabricated structural bridge elements made entirely of UHPC, retrofit and repair of bridge decks, girders, and substructures, and field-cast connections between prefabricated bridge elements (PBEs). This last application is currently the most popular within the United States and Canada and has proved to be a common entry point for many owners new to this technology.

## **PROBLEM STATEMENT AND OBJECTIVE**

The first U.S. deployment of UHPC as a bridge deck overlay was completed in May 2016 on a reinforced concrete slab bridge located in Brandon, IA, in Buchanan County. This bridge is the focal point of this report and is referred to as the “Laporte Road bridge.” A few months after installing the UHPC overlay, a field inspection of the Laporte Road bridge identified some locations along the deck where delamination might have occurred. These locations were identified by sounding the deck using a chain drag. However, it was not known whether delamination, if actually present, occurred at the interface between the UHPC overlay and substrate concrete, within the existing concrete deck, or within the UHPC overlay itself. It was noted, prior to installing the overlay, that there were some regions on the deck where the existing concrete appeared distressed and where corrosion of steel had caused delamination. Thus, there was a need to assess the bond between the UHPC overlay and substrate concrete and determine whether locations of potential delamination were a result of poor bond between the UHPC overlay and the concrete deck or a result of pre-existing issues.

These delamination mechanisms are illustrated in figure 3, which depicts a concrete bridge deck with a UHPC overlay. Delamination due to debonding between the UHPC overlay and the existing deck concrete might be caused by poor surface preparation of substrate concrete, poor consolidation of UHPC, excessive tensile stress normal to the material interface, or excessive shear stress parallel to the material interface. Delamination within the existing concrete deck would likely be caused by corrosion-induced spalling of cover concrete or freeze-thaw damage and could have preceded the UHPC overlay. Delamination within the UHPC overlay layer is possible, but highly unlikely.

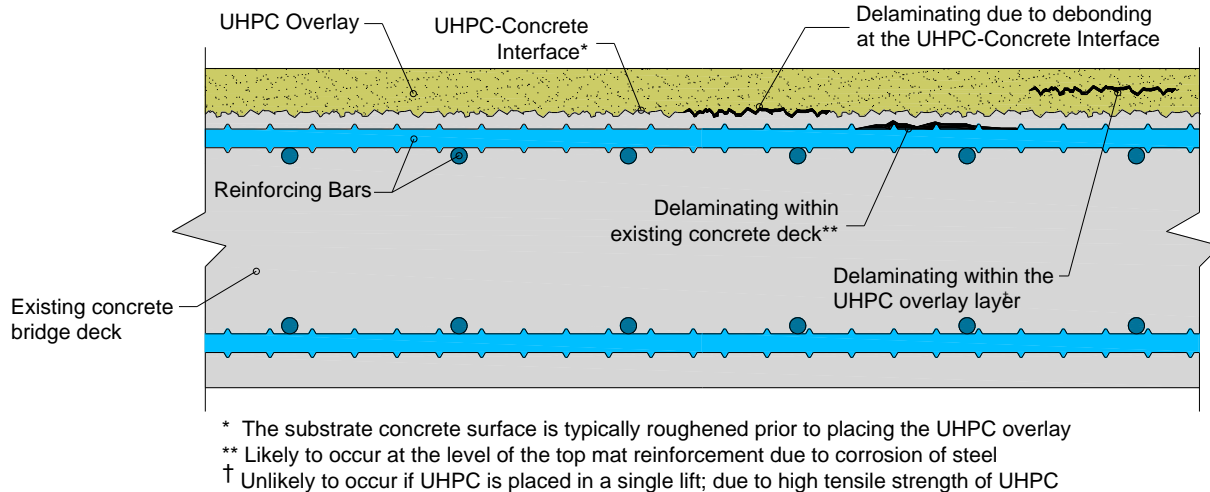


**Figure 3. Illustration. Existing concrete bridge deck with a UHPC overlay and potential locations of delamination.**

## APPROACH

In November 2016, researchers from the Federal Highway Administration’s (FHWA) Turner-Fairbank Highway Research Center (TFHRC) conducted a field study on the Laporte Road bridge to evaluate the bond between the UHPC overlay and the substrate concrete bridge deck. The approach included synthesis of photographic evidence, a field inspection of the bridge deck surface using a chain drag, physical testing of the UHPC-concrete interface bond according to American Society of Testing and Materials (ASTM) C1583—the direct tension bond pull-off test—and visual inspection of the UHPC-concrete interface using scanning electron microscopy.

## REPORT OUTLINE

This report is divided into five chapters. Chapter 1 provides an introduction to the problem and the approach taken by the research team. Chapter 2 provides an overview of UHPC-class materials and their properties, and discusses some previous research on UHPC overlays and previous field deployments. Chapter 3 describes the Laporte Road Bridge, overlay installation, and some key observations prior to installation of the overlay. Chapter 4 describes the methodology used to develop a test plan and the details of the bond test method. Lastly, chapters 5 and 6 provide results and conclusions, respectively.



## CHAPTER 2. BACKGROUND AND PREVIOUS RESEARCH

### PROPERTIES OF UHPC-CLASS MATERIALS

Typically, UHPC-class materials are composed of portland cement, supplementary cementitious materials (SCM) such as silica fume, fine sand, silica powder, high volumes of chemical admixtures to promote flow, and high volumes of fiber reinforcement. Gradation of solids found in UHPC is engineered to produce a dense matrix with a discontinuous pore structure, which results in exceptional durability, high stiffness, compressive strengths greater than 21.7 ksi (150 MPa), and tensile strengths higher than conventional concrete-like materials. Most UHPCs deployed in structural applications use high-strength steel microfiber reinforcement, and the percentage of fibers per unit volume of material is typically equal to or greater than two percent. This allows UHPC-class materials to undergo large tensile deformations prior to loss of tensile capacity. That is, UHPC exhibits post-cracking load-carrying capacity and tensile ductility. Finally, most UHPCs are designed to be self-consolidating and flowable under gravity without mechanical assistance.

Currently, no definition of UHPC is universally accepted, and the specific properties that define this class of materials are still being debated. FHWA's definition does, however, provide some insight into the constituents and properties of UHPC-class materials. FHWA defines UHPC as:

a cementitious composite material composed of an optimized gradation of granular constituents, a water-to-cementitious materials ratio less than 0.25, and a high percentage of discontinuous internal fiber reinforcement. The mechanical properties of UHPC include compressive strength greater than 21.7 ksi (150 MPa) and sustained post-cracking tensile strength greater than 0.72 ksi (5 MPa). UHPC has a discontinuous pore structure that reduces liquid ingress, significantly enhancing durability compared to conventional concrete. (Graybeal 2011)

Finally, like conventional concretes, UHPC properties are highly dependent on the curing environment. UHPCs subjected to heat and/or steam during curing tend to exhibit enhanced mechanical and durability properties compared with UHPCs cast in the field; these are referred to as "field-cast" UHPCs. (Graybeal 2006; Graybeal and Stone 2012)

Table 2 lists typical properties of field-cast UHPC. The data shown in this table was collected through a series of research projects executed at the FHWA TFHRC. (Graybeal 2006; Graybeal and Stone 2012; Graybeal and Baby 2013; Swenty and Graybeal 2013)

**Table 2. Typical properties of field-cast UHPC.**

<b>Material Characteristic</b>	<b>Average Result</b>
Density	155 lb/ft <sup>3</sup> (2,480kg/m <sup>3</sup> )
Compressive strength (ASTM C39; 28-day strength)	24 ksi (165 MPa)
Modulus of elasticity (ASTM C469; 28-day modulus)	7,000 ksi (48 GPa)
Direct tension cracking strength (uniaxial tension with multiple cracking)	1.2 ksi (8.5 MPa)
Split cylinder cracking strength (ASTM C496)	1.3 ksi (9.0 MPa)
Prism flexural cracking strength (ASTM C1018; 12 in (305-mm) span)	1.3 ksi (9.0 MPa)
Tensile strain capacity before crack localization and fiber debonding	>0.003
Long-term creep coefficient (ASTM C512; 11.2 (77 MPa) load)	0.78
Long-term shrinkage (ASTM C157; initial reading after set)	555 microstrain
Total shrinkage (embedded vibrating wire gage)	790 microstrain
Coefficient of thermal expansion (AASHTO TP60-00)	8.2 x10 <sup>-6</sup> in/in/°F (14.7 x10 <sup>-6</sup> mm/mm/°C)
Chloride ion penetrability (ASTM C1202; 28-day test)	360 coulombs
Chloride ion penetrability (AASHTO T259; 0.5-in (12.7-mm) depth)	<0.10 lb/yd <sup>3</sup> (<0.06 kg/m <sup>3</sup> )
Scaling resistance (ASTM C672)	No scaling
Abrasion resistance (ASTM C944 2x weight; ground surface)	0.026 oz. (0.73 g) lost
Freeze-thaw resistance (ASTM C666A; 600 cycles)	RDM = 99 percent
Alkali-silica (ASTM C1260; 28-day test)	Innocuous

RDM = Relative dynamic modulus of elasticity; ASTM = American Society of Testing and Materials;  
AASHTO = American Association of State Highway and Transportation Officials.

## UHPC AS A BRIDGE DECK OVERLAY MATERIAL

Bridge decks are commonly rehabilitated using overlays depending on the cause of deck deterioration, available budget, and desired service life of the rehabilitated structure. Common overlay materials include conventional concrete, high-performance concretes (HPCs), latex-modified concretes (LMCs), asphalt, and polymer-based materials. There are two common methods for installing a traditional bridge deck overlays: 1) without removal of cover concrete; or 2) after full or partial removal of cover concrete. When the cover concrete remains intact, localized damage to the deck may be repaired prior to placing the overlay, and the deck may be milled or roughened to promote bonding between the deck and the overlay. When the second technique is employed, cover concrete is removed by hydrodemolition, milling or other mechanical means; in previous deployments, most UHPC overlays were placed using this second method. The performance objectives of a bridge deck overlay might include: protecting the underlying deck and reinforcement from contaminants, providing additional strength and stiffness to the deck system, or extending the service life of the overall structure. A number of properties listed in Table 2 make UHPC a viable option for use as a bridge deck overlay material. UHPC overlays offer the following potential advantages:

- UHPC has an excellent low permeability and good resistance to freeze-thaw damage. Thus, the potential for ingress of contaminants and freeze-thaw damage is significantly reduced compared with conventional overlay materials.
- UHPC has good abrasion resistance, which means reduced potential for rutting.
- Compared with conventional concretes, a well-designed UHPC mix exhibits relatively low shrinkage, which reduces the potential for shrinkage-induced cracking. If the UHPC does crack, crack widths are typically significantly smaller than those that would form in a conventional concrete system due to the UHPC's internal microfiber reinforcement.
- UHPC has high strength and high stiffness. Thus, a thin layer could provide both enhanced durability and increased strength with minimal added dead load. Traditionally, rigid concrete overlays range in thickness between 2.5" (51 mm) and 6" (152 mm) (Krauss, Lawler, and Steiner 2009); this results in dead loads between 30 psf (1.4 kN/m<sup>2</sup>) and 75 psf (3.6 kN/m<sup>2</sup>). Previous deployments of UHPC as an overlay, which will be discussed in the following section, have used overlay thicknesses between 1" (25 mm) and 2" (51 mm) (Brühwiler and Denarié 2013); this results in dead loads between 12 psf (0.57 kN/m<sup>2</sup>) and 26 psf (1.2 kN/m<sup>2</sup>).
- UHPC bonds well to existing concrete surfaces if the proper surface preparation is applied, such as using an exposed aggregate or roughened surface finish. (De La Varga, Haber, and Graybeal 2017)

The primary difference between typical UHPC formulations and UHPCs that have been specially formulated for overlay applications are rheological properties. As noted above, most UHPCs are formulated to flow under the force of gravity. That is, although UHPC is viscous, it has a low fluid yield stress, which allows that material to flow freely under gravity. UHPCs for overlay applications are typically formulated to be thixotropic. Thixotropy is a time-dependent shear thinning property of a non-Newtonian fluid. A thixotropic material will remain solid-like under static conditions and will flow when agitated or sheared. This is an important property to note because bridge decks are not level. Thus, if a typical (nonthixotropic) UHPC is used as a bridge deck overlay, it will flow from the crown, or high side, of the super elevation to low points on the structure.

Figure 4 and figure 5 compare the flow table test (ASTM C1437) response of typical, nonthixotropic UHPC and thixotropic UHPC that was specially formulated for bridge deck overlays. (ASTM C1437-15 2015) Once the miniature slump cone was removed, the nonthixotropic UHPC spread across the flow table, while the thixotropic UHPC remained in solid-like state.



**Figure 4. Photo. Nonthixotropic formulation.**



**Figure 5. Photo. Thixotropic formulation.**

Other than the difference in rheological properties, the two formulations were similar in regard to mechanical and durability properties. For example, figure 6 shows a comparison of direct tension behavior of two UHPCs with nearly identical formulations, except that one was formulated to be thixotropic; the direct tension test method is shown in figure 7. (ASTM C1583/C1583M-13 2013) The materials exhibit similar elastic stiffness and post-cracking tensile ductility. Further, figure 8 shows a comparison of the same two UHPC materials and their associated bond strength to existing concrete measured according to ASTM C1583 (figure 9). (ASTM C1583/C1583M-13 2013)

The data shown reflect bond strength of UHPC bonded to an existing concrete surface that was roughened (using an exposed aggregate treatment) prior to placement of UHPC. Both UHPC materials exhibited similar bond strength despite having different rheology.

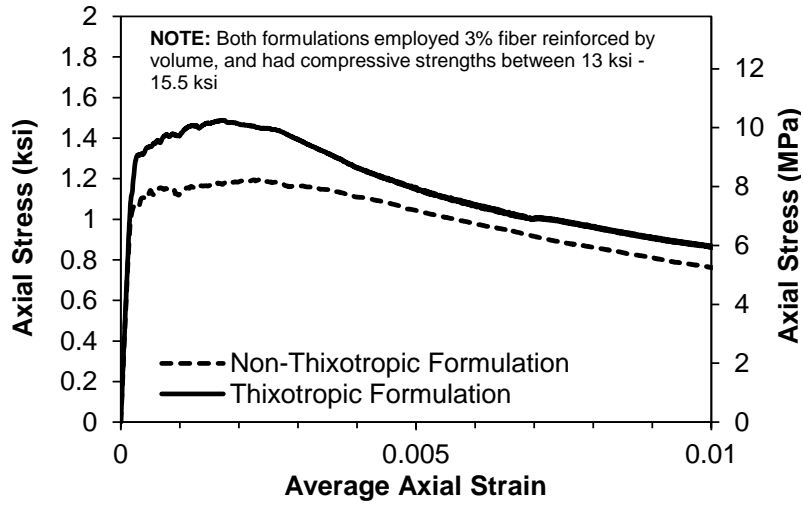


**Figure 6. Graph. Comparison of the direct tension behavior of thixotropic and nonthixotropic UHPC.**

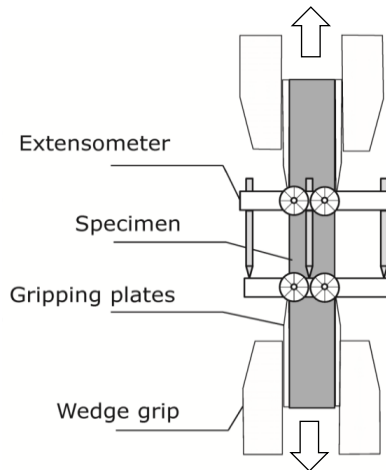


**Figure 7. Illustration. Direct tension test method for UHPC.**

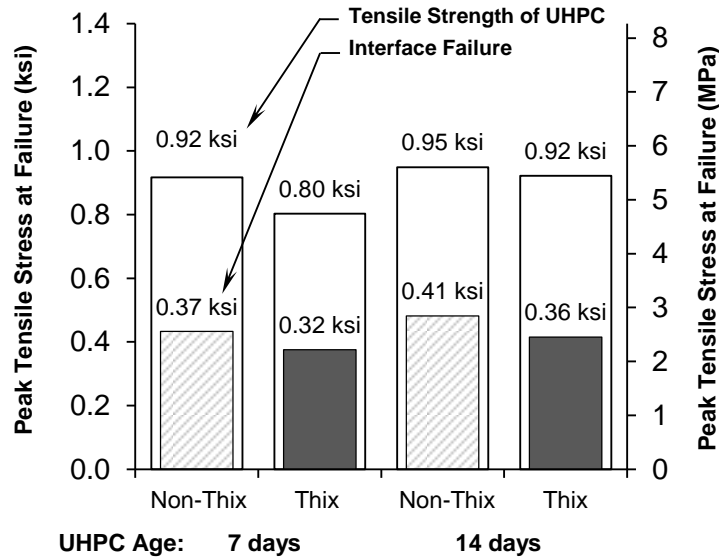


**Figure 8. Graph. Comparison of the direct tension bond strength of thixotropic (Thix) and nonthixotropic (Non-Thix) UHPC formulations.**

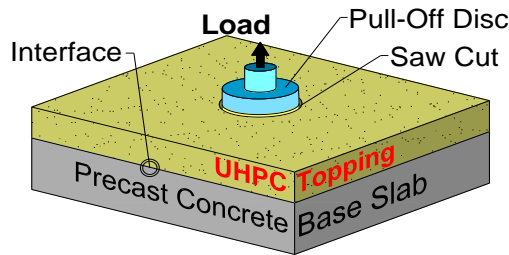


**Figure 9. Illustration. ASTM C1583—Direct tension bond pull-off test method.**

The cost of UHPC is generally higher than most highway bridge construction materials. Further, the material cost and bid line-item cost for UHPC-class materials can differ substantially. The Federal Highway Administration (FHWA) provides high-quality information to serve Government, industry, and the public in a manner that promotes public understanding. Standards and policies are used to ensure and maximize the quality, objectivity, utility, and integrity of its information. FHWA periodically reviews quality issues and adjusts its programs and processes to ensure continuous quality improvement compares the approximate cost of various overlay solutions. The UHPC costs shown reflect only material costs but not associated installation costs and are thus relatively low. In general, the cost of UHPC overlays in the United States will likely be higher than most traditional overlay solutions until the technology becomes established. In Switzerland, UHPC overlays are commonly deployed, and, therefore, costs are becoming competitive.

Table 3 lists the approximate cost ranges of a UHPC on a signature bridge structure, the Chillon Viaduct, in Switzerland; this cost is comparable to the upper-end cost of some conventional solutions.

**Table 3. Approximate cost ranges of bridge deck overlay solutions.**

Overlay Type	Overlay Thickness—in (mm)	Cost—\$/ft <sup>2</sup> (\$/m <sup>2</sup> )
High-performance concrete*	1–5 (25–127)	17–25 (183–269)
Low slump concrete*	1.5–4 (38–102)	13–19 (140–204)
Latex-modified concrete*	1–5 (25–127)	18–39 (193–419)
Asphalt with a Membrane*	1.5–4 (38–102)	3–8 (32–86)
Polymer-based*	0.13–6 (3–152)	10–17 (107–183)
Nonproprietary UHPC	1–2 (25–52)	3–6 (32–64)†
Proprietary UHPC		9–18 (97–184)‡
<b>Rehabilitation of the Chillon Viaduct (Switzerland)</b>		
Proprietary UHPC Overlay	1.6 (40)**	20 (215)**
<b>Other Rehabilitation Solutions</b>		
Deck Replacement*	—	43 - 53 (462–570)

\*Data collected from Krauss et al. (2009); The costs shown reflect average values from low and high ranges.

\*\*Data collected from Brühwiler et al. (2015); Price reflects cost of material and installation.

†Price reflects material cost only; Assumes UHPC CY cost of \$1,000.

‡Price reflects material cost only; Assumes UHPC CY cost of \$3,000.

—Not applicable.

## PREVIOUS UHPC OVERLAY RESEARCH AND DEPLOYMENTS

The concept of using UHPC as an overlay was pioneered in Switzerland and has since been deployed on numerous bridges in Europe. A number of laboratory studies were conducted prior to field deployments. Studies have been conducted on the flexural and combine flexure-shear behavior of reinforced concrete (RC) members with thin UHPC overlays. (Habel, Denarié, and Brühwiler 2007; Noshiravani and Bruhwiler 2013)

Findings indicated that applying a thin layer of UHPC, 1.25- to 4-in(32- to 102-mm) thick, to an existing reinforced concrete member to form a composite UHPC-RC member can increase stiffness, decrease crack width and spacing, and increase load-carrying capacity of the element. Further, results indicated that UHPC-RC elements can achieve composite behavior if the concrete surface was prepared using hydrodemolition prior to casting UHPC.

A study conducted at Iowa State University further investigated the behavior of reinforced concrete slab-like element strengthened using UHPC overlays. (Aaleti, Sritharan, and Abu-Hawash 2013) Sixty slant shear bond tests and three large-scale flexural tests were conducted.

Slant shear tests were used to investigate the effect of existing concrete surface roughness on the bond between UHPC and concrete. Subsequently, large-scale flexural tests were used to investigate the system behavior of the RC member with the UHPC overlay. It was concluded that increasing the surface roughness of the existing concrete increased the bond strength between concrete and the overlay material. It was also concluded that a minimum surface roughness of 0.08-in (2 mm) was required for a reinforced concrete member with a UHPC overlay to achieve good flexural performance.

A study conducted at Michigan Technological University investigated using UHPC as a bridge deck overlay material considering time-dependent effects such as shrinkage and stresses within the system during service. (Shann 2012) A series of restrained ring shrinkage tests were conducted according to a modified version of the American Association of State Highway and Transportation Officials (AASHTO) PP34-99 test method. A parametric study was executed using two-dimensional and three-dimensional finite-element analysis (FEA) to investigate the behavior of a UHPC overlay in bridges with varied girder spacing, overlay thicknesses, support conditions, and bridge deck thicknesses. The influence of relative stiffness between the UHPC overlay and the underlying deck concrete was investigated. A series of HS-20 design truck loading configurations were also considered.

The debonding and interfacial shear stress was found to increase with overlay thickness, while tension stress that would produce cracking or fracture in a UHPC overlay decreased with increased overlay thickness. These effects were largely attributed to shifts in the neutral axis location. The authors concluded that, when effects of restrained shrinkage and live load were combined, the tensile stresses in a UHPC overlay controlled the design. The authors also concluded that UHPC overlays may not be compatible on bridge decks thicker than 10 in (254 mm) due to neutral axis shifting, which causes large tensile stresses in the UHPC overlay.

These results were obtained from a limited FEA study. The majority of results were obtained using a conservative, overly simplified plate model. When an actual bridge structure with a UHPC overlay was analyzed, the interfacial shear and debonding stresses at the UHPC-concrete interface were relatively low.

Researchers have also investigated the use of UHPC as a topping layer on orthotropic steel bridge decks. Research conducted by Toutlemonde et al. studied the feasibility of using a thin layer of UHPC to reduce the potential of fatigue-induced damage and cracking in orthotropic steel decks. (Toutlemonde et al. 2013) Two systems were tested: (1) where a thin layer of UHPC was cast over wire mesh placed atop an orthotropic steel deck specimen; and (2) where a thin layer of UHPC was cast directly onto an orthotropic steel deck specimen that employed short shear studs to improve composite action between the deck and the UHPC overlay. Results showed that imperfect bonding between the steel deck plate and the UHPC topping caused slippage and some cracking at the interface under extremely high loading. Nevertheless, experimental and numerical modeling found that using a UHPC overlay could reduce stresses in the orthotropic steel deck compared to a deck with a bituminous overlay.

Since 2004, UHPC overlays have been deployed on more than 20 bridges in Switzerland and on one bridge in Slovenia. (Brühwiler and Denarié 2013; Sajna, Denarié, and Bras 2012) Applications include waterproofing bridge decks after widening projects, simultaneous

waterproofing and strengthening, and rehabilitation of crash barriers. A detailed summary of these applications is provided by Brühwiler and Denarié. (Brühwiler and Denarié 2013)

The most notable UHPC overlay deployment was in the rehabilitation of the Chillon Viaduct. This 1.34 mi (2.15 km) long elevated bridge structure runs along Lake Geneva in the Swiss canton of Vaud. The viaduct is composed of two parallel post-tensioned concrete box girder structures built in the late 1960s. In 2012, a significant rehabilitation project began, during which inspectors noted that a reinforced concrete deck was exhibiting the initial signs of alkali-aggregate reactivity (AAR). A UHPC overlay was selected to act as both a thin waterproofing layer and a strengthening mechanism. The existing deck was relatively thin—7.1 in (180 mm)—and required a structural strengthening solution that did not cause a significant increase in dead load. A photo of the structure is shown in figure 10, and a typical section is shown in figure 11.



**Figure 10. Photo. Chillon Viaduct: Parallel post-tensioned box girder structures.**

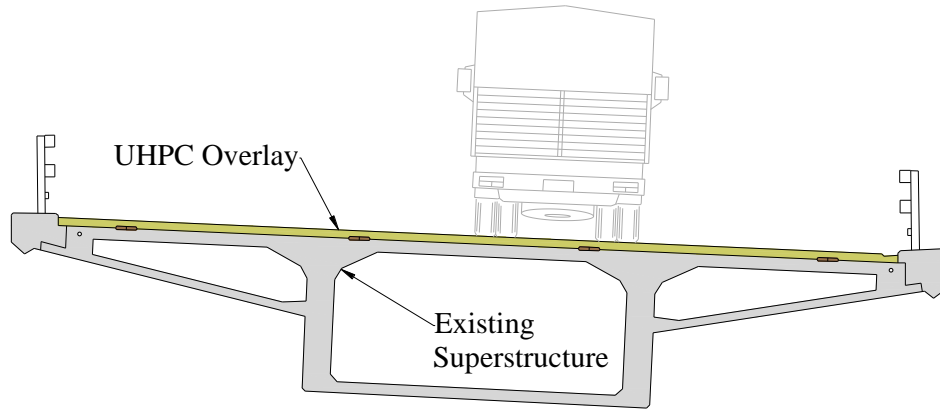


**Figure 11. Illustration. Chillon Viaduct Details: Typical section of a single post-tensioned box girder.**

Figure 12 and figure 13 show photos taken during construction of the Chillon Viaduct UHPC overlay project. The deck rehabilitation was done in two phases completed in the summers of 2014 and 2015—one for each of the two parallel viaduct structures. The UHPC deck overlay for each structure was completed in less than 30 working days. The UHPC overlay, which had a thixotropic formulation, was installed using a specially designed placement machine (shown in figure 13) after completing the UHPC overlay, a 3.2-in (80-mm) asphalt layer was installed as a ride surface.



**Figure 12. Photo. Aerial view of the Chillon Viaduct UHPC overlay construction project.**



**Figure 13. Photo. Placement of UHPC in the Chillon Viaduct project.**



## CHAPTER 3. DETAILS OF THE LAPORTE ROAD BRIDGE

### BRIDGE DESCRIPTION

Constructed in 1960s, the Laporte Road (County Road L) bridge over Mud Creek is a three-span reinforced concrete slab bridge located in Brandon, IA, approximately 35 mi (56.3 km) northwest of Cedar Rapids. A photo of the bridge is shown in figure 14. The bridge was originally designed using H20-44 loading, and although it has low average daily traffic (ADT), it carries large trucks with agricultural loads. The bridge is supported at the ends by reinforced concrete abutments that were cast over steel H-piles. The abutment-to-abutment length of the bridge is 100 ft (30.5 m). The width of the bridge is 28 ft (8.53 m) and services two lanes of traffic.



**Figure 14. Photo. Laporte Road bridge.**

The interior spans of the bridge are supported by H-piles that were permanently encased in concrete. The reinforced concrete slab superstructure of the bridge is composed of three spans that measure 30.5 ft (9.3 m), 39 ft (11.9 m), and 30.5 ft (9.3 m). The slab has a uniform thickness of 16.9 in (430 mm) and was reinforced in the longitudinal direction with bars ranging between #6 and #10 and was reinforced with #6 and #7 bars in the transverse direction. The original design drawings specified a 2-in (51-mm) clear cover between the top mat of steel and the bare ride surface of the concrete deck. The bridge deck has a five percent super elevation.

The bridge deck was beginning to exhibit delaminations and spalling along the northern (low elevation) curblin and at each end at the expansion joints. It is likely that the deterioration was related to chloride laden water ingress into the concrete and past the strip seal expansion joints, leading to reinforcement corrosion and freeze-thaw cycle-related distress. This deterioration had progressed to the point where maintenance actions were necessary. A UHPC overlay solution





**Figure 16. Photo. Distressed region observed on the westbound lane over the pier 1 prior to installing the UHPC overlay.**



**Figure 17. Photo. Distressed region observed on the westbound lane near west abutment prior to installing the UHPC overlay.**

## **OVERLAY INSTALLATION AND FINISHING**

As noted above, the existing surface of the deck was ground to remove poor concrete and provide a roughened surface to promote bond between the concrete substrate and the UHPC overlay material. A photo of the deck surface after scarification is shown in figure 18. On completion of the grinding, all fines and debris were to be removed from the surface of the deck, and deck surface was premoistened a few hours prior to installing the overlay.



**Figure 18. Photo. Deck surface after scarification.**

The UHPC overlay material was mixed in large pan-style mixers. Two mixers were used to provide a constant supply of UHPC; one mixer was discharged while the other was being charged. The UHPC overlay material was then transported and placed using a motorized buggy (shown in figure 19). Workers using a hand tool assisted the placement of UHPC once discharged from the motorized buggy. As the desired overlay layer thickness was achieved, a lane-wide vibratory screed was progressively drawn down the lane. The placement of UHPC and the vibratory screed are shown in figure 19. Once screeded, a water-based, wax-based concrete curing compound was sprayed on the UHPC overlay surface to prevent dehydration. When the entire lane length was complete, the overlay was covered with a thin plastic sheet (shown in figure 20). The UHPC overlay surface was milled to obtain the desired ride surface (shown in figure 21).



**Figure 19. Photo. Placement of the UHPC overlay on the westbound lane.**



**Figure 20. Photo. Curing of the overlay on the westbound lane.**



**Figure 21. Photo. Completed overlay after deck milling looking eastbound.**

## CHAPTER 4. EVALUATION METHODOLOGY

### INTRODUCTION

Evaluation methodology included synthesis of photographic evidence, a field inspection of the bridge deck surface using a chain drag, physical testing of the UHPC-concrete interface bond according to ASTM C1583—the direct tension bond pull-off test—and visual inspection of the UHPC-concrete interface using scanning electron microscopy.

### IDENTIFICATION OF TEST LOCATIONS

The first step in the evaluation process was to identify regions of potential delamination along with regions where the bond between the UHPC overlay and substrate concrete appeared intact. The goal was to select bond test locations on both westbound and eastbound lanes, which corresponded to the two construction stages of the overlay. In addition, it was critical to assess regions of potential debonding and regions of apparent intact bond. Curblines of the existing bridge deck prior to overlay installation were not scarified. Thus, there was also interest in assessing the bond strength in these regions where the existing concrete was not roughened prior to installing the overlay.

Prior to arriving on site, photographic data collected prior to the overlay installation was analyzed to identify the pre-existing distressed regions. Two of these regions are shown in chapter 3 as figure 16 and figure 17. Approximate locations of these regions were recorded on a scale model of the Laporte Road bridge that was developed using a commercially available computer-aided drafting (CAD) program.

Once onsite, the bridge deck was inspected using a chain drag to identify regions of potential delamination. These regions were marked on the deck and recorded using a global positioning satellite (GPS)-based mobile mapping unit. This data was mapped on the aforementioned CAD drawing of the Laporte Road bridge. A total of eight potential delamination regions were found. Of these eight regions, two were selected for bond testing; one on the west-bound lane and one on the east-bound lane. Three regions exhibiting intact bond between the UHPC overlay and the underlying concrete deck were also selected for bond testing; one on the westbound lane and two on the eastbound lane. The eastbound lane locations included regions with and without scarification prior to the overlay installation.

Figure 22 and figure 23 present the observations, inspection findings, and test locations on the western and eastern sides of the bridge, respectively. Moreover, table 4 lists the findings from the onsite chain drag and details related to each region of interest. Regions of good apparent bond are denoted with a “G,” and regions of potential delamination are denoted with a “B.” Regions of potential delamination were found near the boundaries of the overlay construction stage (i.e., at the longitudinal construction joint or near the approaches) or in close proximity to the distressed regions observed prior to installing the overlay.

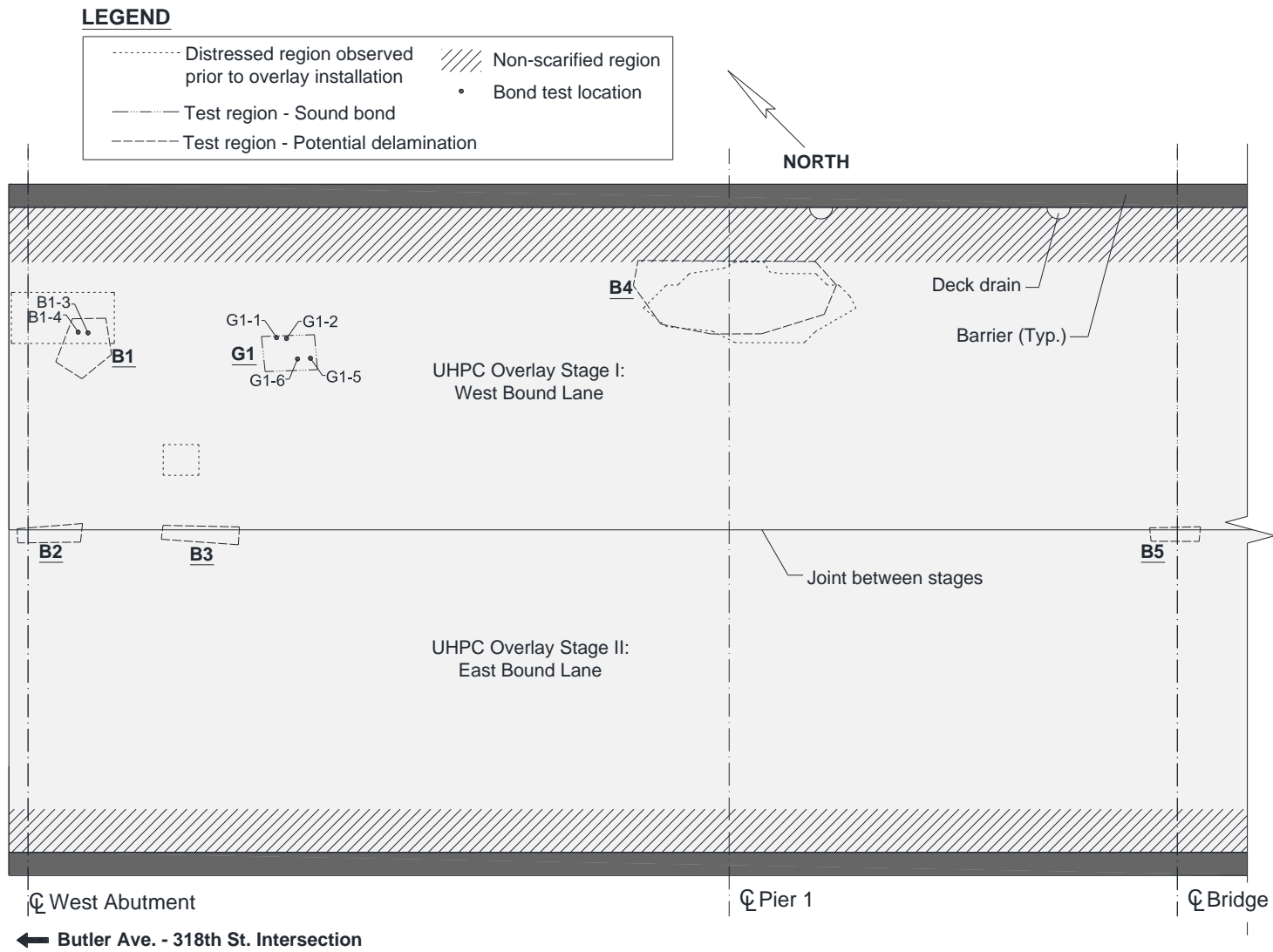
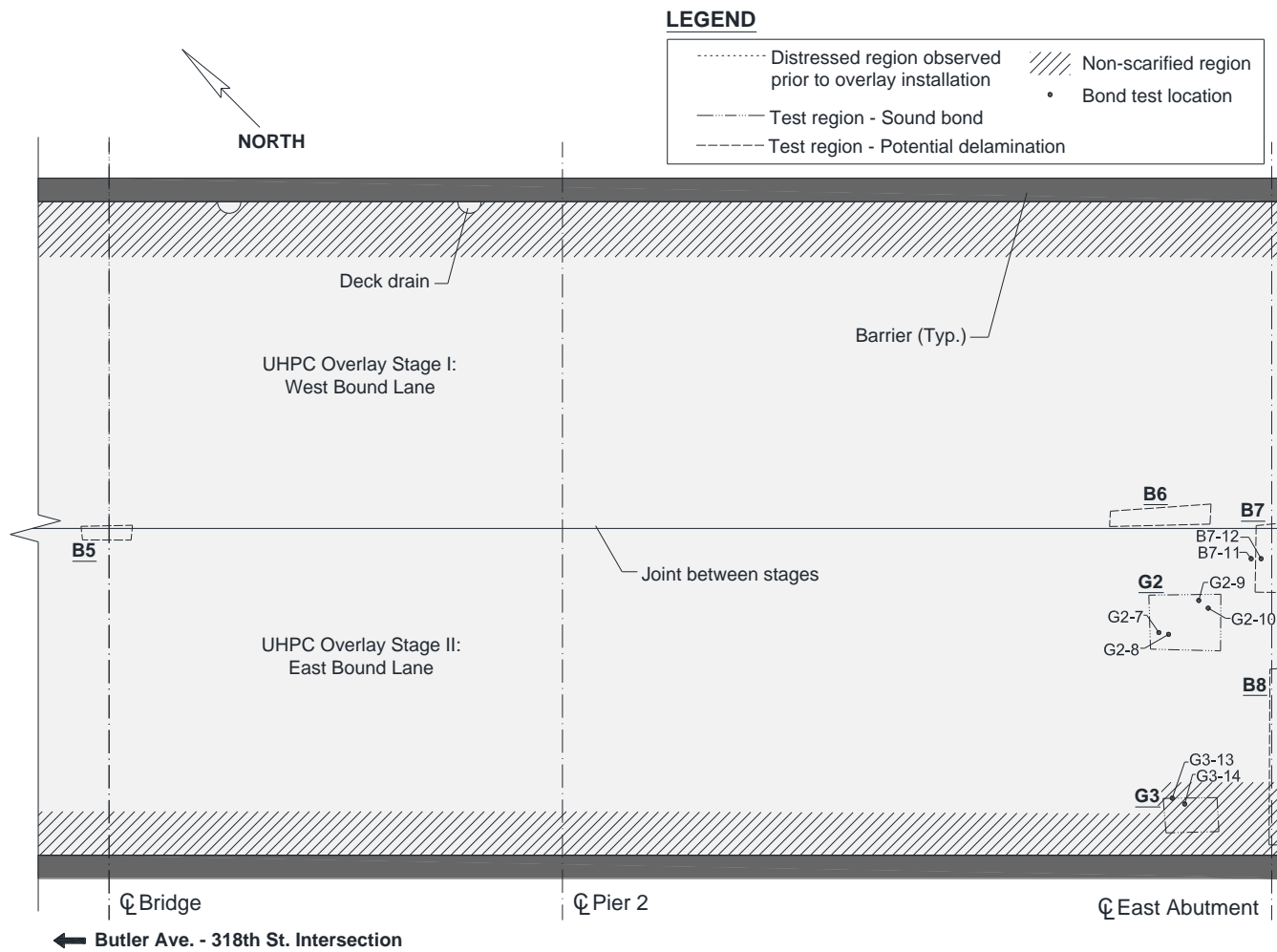


Figure 22. Illustration. Schematic of observations, inspection findings, and test locations on the western side of the bridge.



**Figure 23. Illustration. Schematic of observations, inspection findings, and test locations on the eastern side of the bridge.**

**Table 4. Summary of findings from the chain drag and test location details.**

<b>Location ID</b>	<b>Lane (Construction Stage)</b>	<b>Potential Delamination</b>	<b>Existing Distressed Concrete<sup>†</sup></b>	<b>Scarified Substrate</b>	<b>Bond Testing</b>	<b>Number of Pull-off Tests</b>	<b>SEM Analysis</b>
G1	Westbound (I)	No	No	Yes	Yes	4	No
G2	Eastbound (II)	No	No	Yes	Yes	4	Yes
G3	Eastbound (II)	No	No	No	Yes	2	Yes
B1	Westbound (I)	Yes	Yes	Yes	Yes	2	No
B2	Westbound (I) and Eastbound (II)*	Yes	No	Yes	No	—	—
B3	Westbound (I) and Eastbound (II)*	Yes	No	Yes	No	—	—
B4	Westbound (I)	Yes	Yes	Yes	No	—	—
B5	Westbound (I) and Eastbound (II)*	Yes	No	Yes	No	—	—
B6	Eastbound (II)	Yes	No	Yes	No	—	—
B7	Eastbound (II)	Yes	No	Yes	Yes	2	Yes
B8	Eastbound (II)	Yes	No	Yes	No	—	—

\* Region was along the construction joint between construction stages.

† As determined by photographic evidence.

—Not applicable.

## **BOND TESTING**

The interface bond strength between the existing concrete deck and the UHPC overlay material was assessed using the direct tension bond pull-off test method. A schematic of this test, which was conducted according to ASTM C1583 (ASTM C1583/C1583M-13 2013), is shown in figure 24.

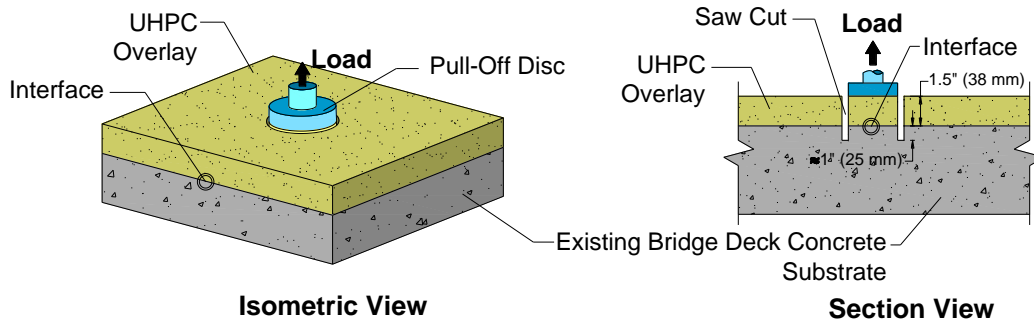


**Figure 24. Illustration. Direct tension pull-off bond test based on ASTM C1583.**

This test was prepared by first gluing a 2-in (51-mm) diameter steel pull-off disc to the bonded material at the desired test location; here, the “bonded” material is the UHPC overlay, and the substrate is the underlying deck concrete. Prior to gluing the pull-off disc, the bonded surface was roughened to promote bonding between the steel disc and the UHPC overlay. Once the adhesive layer cured, a partial core was drilled through the bonded material and into the substrate material. This ensured that the load path passed directly through the interface between the two materials. For this project, the substrate core depth was approximately 1 in (25 mm) as shown in figure 24. A specialized pull-off test fixture was then used to apply load and record data according to the ASTM C1583 standard. Tensile load was applied to the steel disc at a constant rate of  $5 \pm 2$  psi/sec ( $34.5 \pm 13.8$  kPa/sec) until failure. The failure load and failure mode were recorded on completion of the test. The nominal tensile stress could then be calculated.

Typically, failure occurred by one of four modes, which are shown in Figure 25. These photos were taken from previous projects where this test was employed. If Mode 2 failure occurred (Figure 25-B) the true bond strength between the two materials could be assessed. If Mode 1 (Figure 25-A) or 3 (Figure 25-C) occurred, the tensile strength of the failing material could be assessed and the interface bond strength recognized to be higher than the tensile stress achieved. Finally, if Mode 4 failure occurred (Figure 25-D), the interface bond strength could be recognized to be higher than the tensile stress achieved.



A. Mode 1: Substrate failure.

B. Mode 2: Bond failure at the interface.

C. Mode 3: Failure in the bonded material.

D. Mode 4: Failure in the disc adhesive.

**Figure 25. Photos. Failure modes associated with the direct tension pull-off bond test; photos taken from previous projects.**

These tests were completed over the course of two days in November 2016. On day one, air temperature was between 40°F (4.5°C) and 50°F (10°C), and the bridge deck surface was damp. On day two, air temperature was also the between 40 °F (4.5°C) and 50°F (10°C), but the deck surface was dry. A specially formulated two-part adhesive was used to secure the pull-off disc to the UHPC overlay. A heat gun was used to dry the deck surface prior to pull-off disc installation and was also used to accelerate adhesive curing (shown in figure 26). Figure 26 and Figure 27 show photos from test preparation and the bond testing, and figure 28 shows a set of samples after testing.



**Figure 26. Photo. In-situ bond testing on the Laporte Road bridge.**

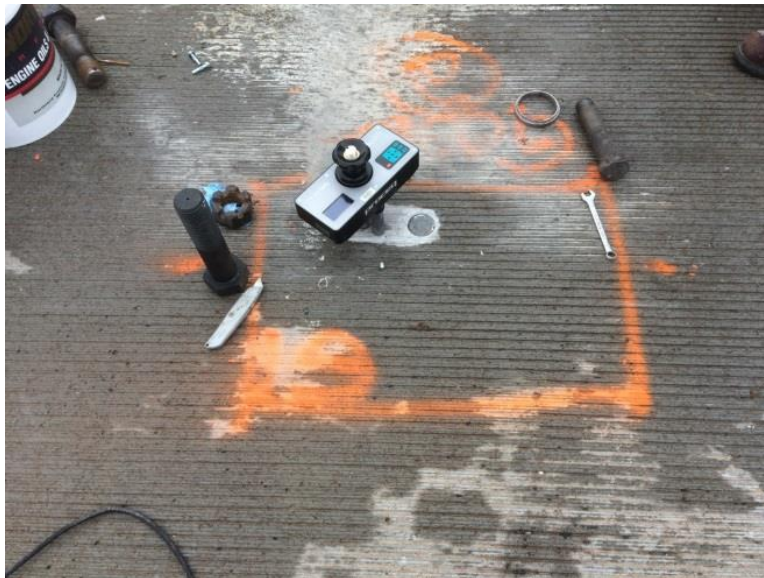


**Figure 27. Photo. Preparation of the bond test location on the Laporte Road bridge.**



**Figure 28. Photo. Two test samples after failure in the substrate concrete.**

## **SCANNING ELECTRON MICROSCOPY**

After onsite bond testing, all cores were brought to TFHRC for documentation and potential future testing. Three bond test specimen cores were selected for detailed microstructural analysis using a scanning electron microscope (SEM). The goal of microstructural analysis was to further investigate the interface between the UHPC overlay and the substrate concrete deck. Selected cores were taken from test locations G2, G3, and B7 as noted in table 4. To prepare SEM specimens, 1.77-in by 1-in (45-mm by 25-mm) samples were cut from each of the three cores of interest; each sample included the interface between the two materials. These samples were immersed in isopropanol for 48 hours, dried in a vacuum oven at 77 °F (25°C), impregnated with epoxy resin, lapped, and polished to a surface roughness of 0.25  $\mu\text{m}$ .

Microstructural analysis of the selected interface samples was done using a FEI Quanta 650 SEM equipped with a concentric backscatter detector. The microscope was operated under high vacuum at 15 KV and with a 0.39-in (10 mm) working distance. Large backscatter electron (BSE) mapping areas were collected using Aztec 2.4 EDS microanalysis software. The entire surface of the interface was mapped at two magnifications. First, a magnification of 150x was selected to obtain a general view of the fiber and entrapped air distributions near interface, referred as “General” maps. Under this magnification, the entire interface was mapped with two General maps measuring approximately 0.9-in by 0.26-in (23.0 mm by 6.5 mm). The interface was mapped a second time with 1500x magnification to analyze distribution of porosity, aggregate, unhydrated cement particles, and UHPC hydration products in proximity to the UHPC-concrete interface. These maps are referred as “Quantitative” maps. Five Quantitative maps measuring approximately 0.31-in by 0.1-in (8.0 mm by 2.5 mm) were required to fully map the interface at the 1500x magnification.

The interface was analyzed in consecutive 10- $\mu\text{m}$ -wide bands, starting from the location where UHPC’s cement paste contacted the concrete deck substrate. This is illustrated in figure 29. This analysis was conducted 10 times, moving backward into the bulk of the UHPC paste (100  $\mu\text{m}$

away from the interface line). A similar process was used to characterize the interfacial transition zone in cement-based materials. (Diamond and Huang 2001; Elsharief, Cohen, and Olek 2003) This process is currently being used by researchers at TFHRC to characterize bond between fresh cementitious materials and existing concrete, and was previously used by Beushausen, Höhlig, and Talotti (2017) to characterize the microstructure of bonded concrete overlays.

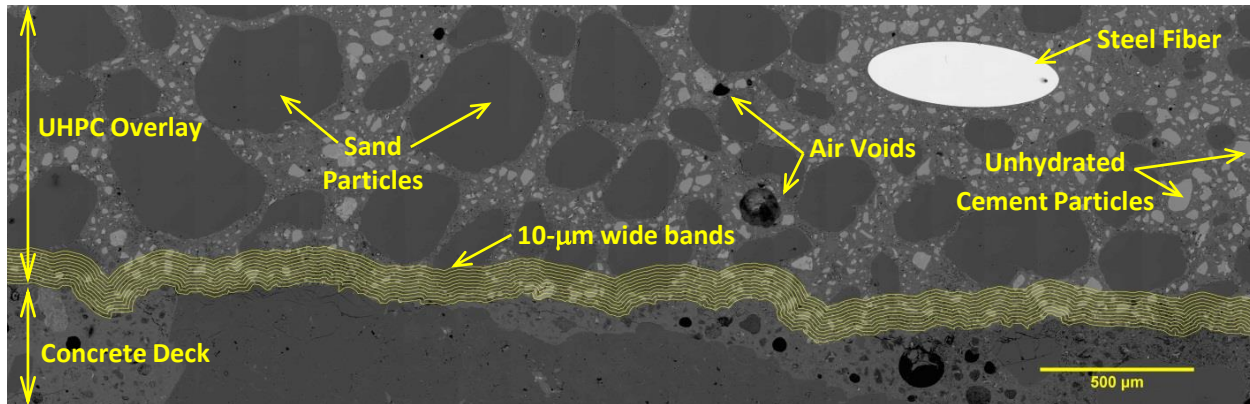


**Figure 29. Illustration. Example of segmentation process on Quantitative map with 10- $\mu$ m-wide bands used to study the distribution of porosity, aggregate, and unhydrated cement particles of the UHPC-concrete interface.**

Image analysis software ImageJ 1.49v1 was used to measure porosity, aggregate, and unhydrated cement particles in each of the 10- $\mu$ m-wide bands. The result of this analysis is a quantitative measure of the porosity, aggregate, hydration products, and unhydrated cement particle content near the interface. Specific details of the process to measure porosity are described in Beyene et al. (2017).

## CHAPTER 5. RESULTS AND DISCUSSION

A summary of results from bond testing is shown in table 5. Fourteen bond tests were completed. Specimens exhibited 1 of 2 failure modes: Mode 1, which is failure in the substrate, or Mode 4, which is failure in the adhesive layer between the test disc and the UHPC overlay. Results are presented in three groups: (1) test locations G1 and G2; (2); test location G3; and (3) test locations B1 and B7.

**Table 5. Summary of results from bond testing.**

Location ID	Sample	Test Day	Lane	Potential Delamination	Scarified Surface	Peak Stress, psi (MPa)		Failure Mode	Interface Condition <sup>c</sup>
G1	1	1	West-bound	No	Yes	248.6	(1.71)	4	Bond appeared intact
	2					420.3	(2.90)		
	5					394.5	(2.72)		
	6					270.1	(1.86)		
G2	7	2	East-bound	No	Yes	286.7	(1.98)	4	Bond appeared intact
	8					290.2	(2.00)		
	9					233.9	(1.61)		
	10					182.9	(1.26)		
G3	13	2	East-bound	No	No	474.6	(3.27)	1	Bond appeared intact
	14					344.6	(2.37)		
B1	3	1	West-bound	Yes	Yes	— <sup>a</sup>		1 <sup>b</sup>	Bond appeared intact
	4					114	(0.79)	1	
B7	11	2	East-bound	Yes	Yes	35.7	(0.25)	1	Bond appeared intact
	12					— <sup>a</sup>		1 <sup>b</sup>	

<sup>a</sup>Load was not applied to the specimen; the core was loose after coring, and could be removed freely.

<sup>b</sup>Delamination was present within the concrete substrate.

<sup>c</sup>Interface condition based on visual inspection upon core removal.

—Not applicable.

### TEST LOCATIONS G1 AND G2

Specimens tested from region G1 and G2, which represented a test location with no indication of delamination and scarification prior to placement of the UHPC overlay, all failed in the adhesive between the test disc and the UHPC overlay (Mode 4). Peak stresses recorded prior to failure were between 182.9 psi (1.26 MPa) and 420.3 psi (2.90 MPa). Figure 30 shows a set of test discs removed from G1 and G2 samples. The figure shows the face of the disc that was bonded to the UHPC overlay. Portions of the failure are seen in the UHPC and at the interface between the adhesive and the UHPC.

Specimens failing in Mode 4 were subsequently removed from the test location by applying a prying action to the sample using a hand tool. In each case, the prying action resulted in fracture of the substrate concrete. Figure 30 and Figure 31 show a representative sample (G2-9) from the G1 and G2 test locations. The bond between the UHPC overlay and the substrate concrete appears intact.



**Figure 30. Photo. Test disc removed from samples from G1 and G2 locations.**



A. Front of G2-9 specimen after testing.

B. Back of G2-9 specimen after testing.

C. UHPC-concrete interface of G2-9 specimen after testing.

**Figure 31. Photos. Specimen G2-9 after testing.**

Figure 32 shows the core location from which sample G2-9 was removed. As expected, apparent damage or delamination in the deck concrete or at the UHPC-concrete interface was not present.

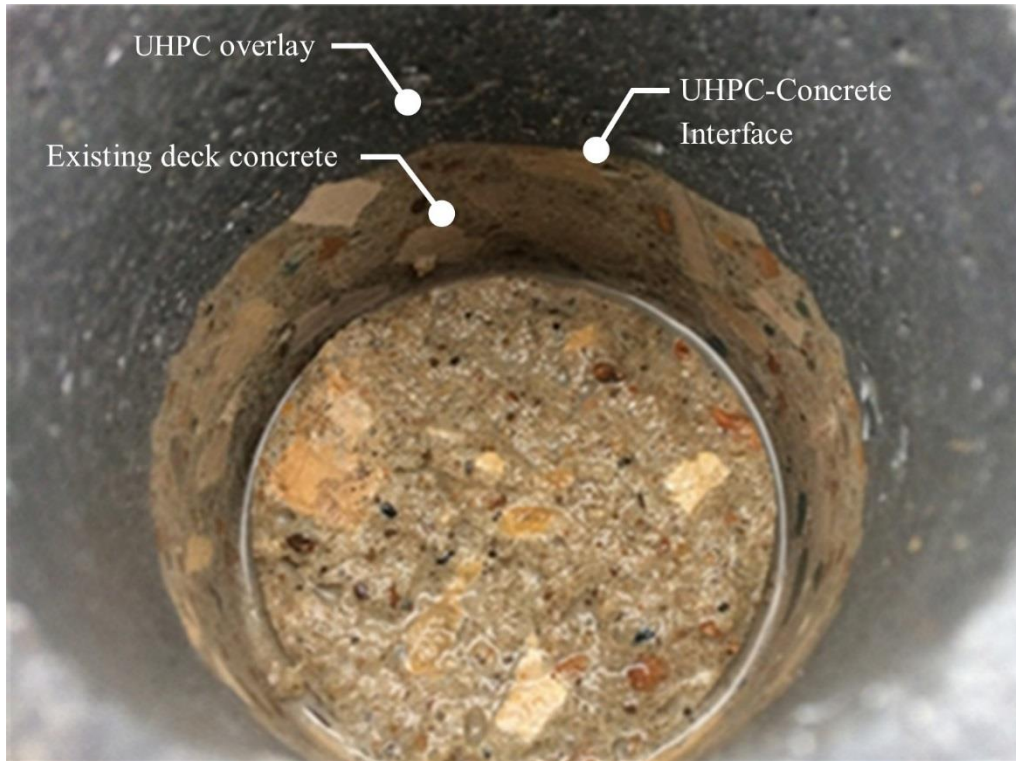


**Figure 32. Photo. Core location for specimen G2-9.**

The microstructural analysis revealed findings that were complementary to data gathered by pull-off testing and visual inspection of test samples. The initial observations from the General map of the G2-8 specimen (shown in Figure 33) revealed the absence of steel fibers in direct contact with the concrete substrate. The width of the UHPC paste band in proximity to the interface exhibiting an absence of steel fibers varied from 0.015 in (0.4 mm) up to 0.09 in (2.4 mm). Roughness induced by the scarification is also visible on the General map by the “valley-hill” configuration of the surface of the concrete deck where the UHPC overlay was deposited.

The General map shown in figure 33 displays a sound interface with close physical contact between hydrated phase of UHPC and the existing concrete deck substrate. This observation is justified by the absence of a gap dividing the paste from the concrete substrate and the presence of hydrated cement products—most likely calcium silicate hydrated (C-S-H) and portlandite—on the interface. The high degree of direct contact between the UHPC overlay and the concrete substrates justifies the relatively high tensile stresses sustained during bond strength testing and the absence of failure at the interface. However, this direct contact between hydrated products of the UHPC overlay and the concrete substrate was locally disrupted by the presence of entrapped air, (shown in figure 34) or poor consolidation or accumulation of debris, which is shown in figure 35. The presence of these features near the UHPC-concrete interface was marginal and did not compromise the overall bond performance.

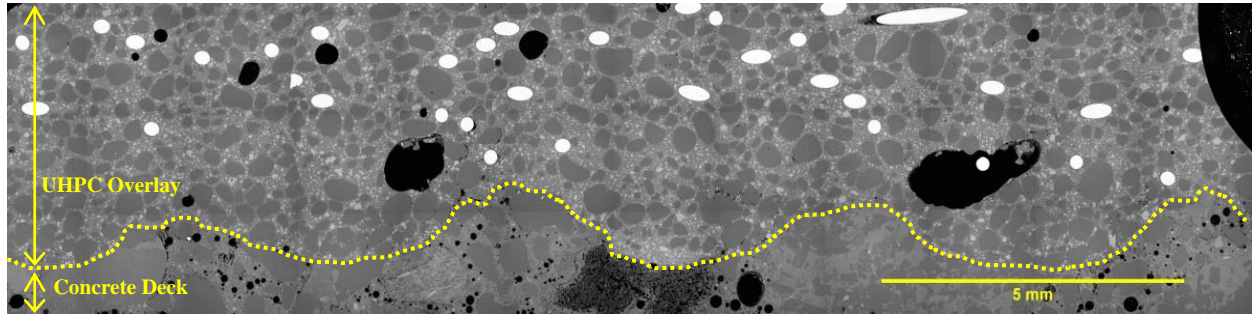


**Figure 33. Electron Microscope Image. General map of the UHPC-concrete interface for specimen G2-8.**

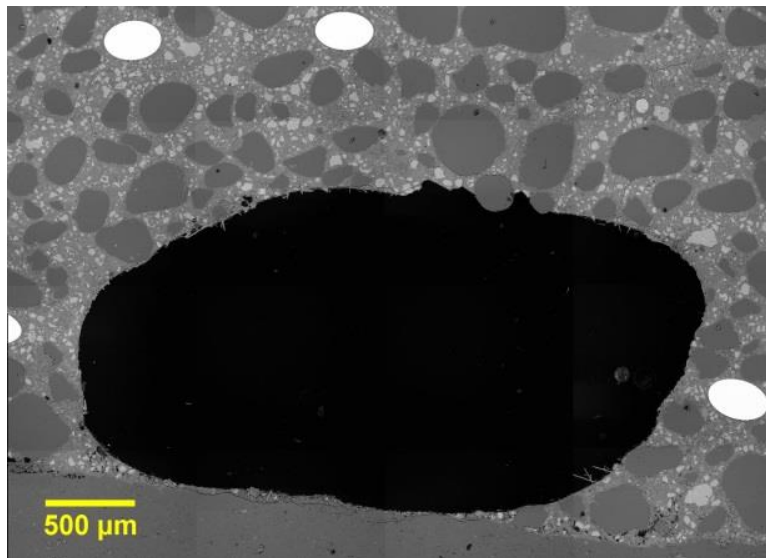


**Figure 34. Electron Microscope Image. BSE image of a void between the UHPC overlay and the substrate concrete.**

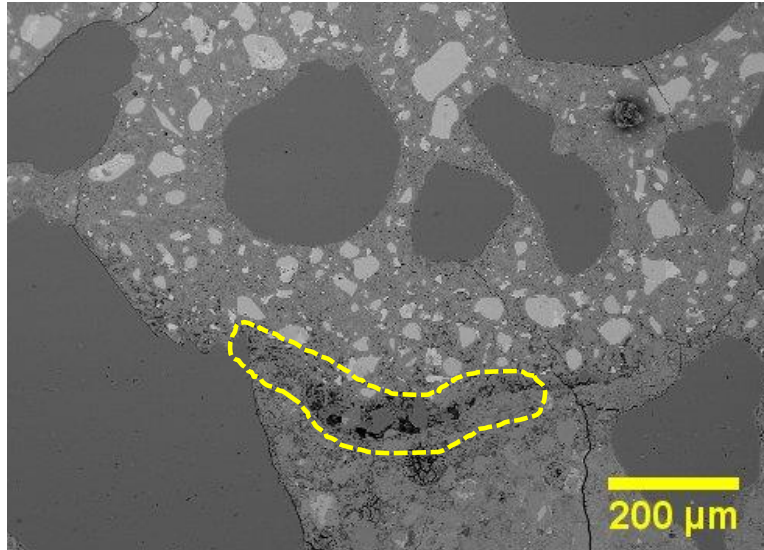


**Figure 35. Electron Microscope Image. BSE image of poor consolidation or debris accumulation at the interface.**

Distribution of the porosity, aggregate, unhydrated, and hydrated cement particles on the UHPC overlay as a function of the distance from the concrete surface is presented in figure 36. This graph shows a high content of hydrated products, above 80 percent, at the interface (from 0- to 10- $\mu\text{m}$  distance). The percentage of hydrated products was reduced as the distance from the interface increased. This diminishing percent of hydrated products was caused by an increase of the aggregate content in the UHPC paste. At approximately 90- $\mu\text{m}$  distance from the interface, the content of both hydrated and aggregate stabilized at from 46 and 40 percent, respectively. This effect has been observed in other types of overlays, and it is associated with reduction in the packing efficiency of the UHPC paste in the vicinity of the concrete surface, also known as “wall-effect.” (Garboczi and Bentz 1991; Ollivier, Maso, and Bourdette 1995; Scrivener, Crumbie, and Laugesen 2004; H Beushausen and Gillmer 2014) The inflexion point on the content of phases, hydrated product, and aggregates at 90- $\mu\text{m}$  distance from the surface is depicted in figure 36 with a vertical dashed red line that marks the extent of wall effect on the UHPC paste.

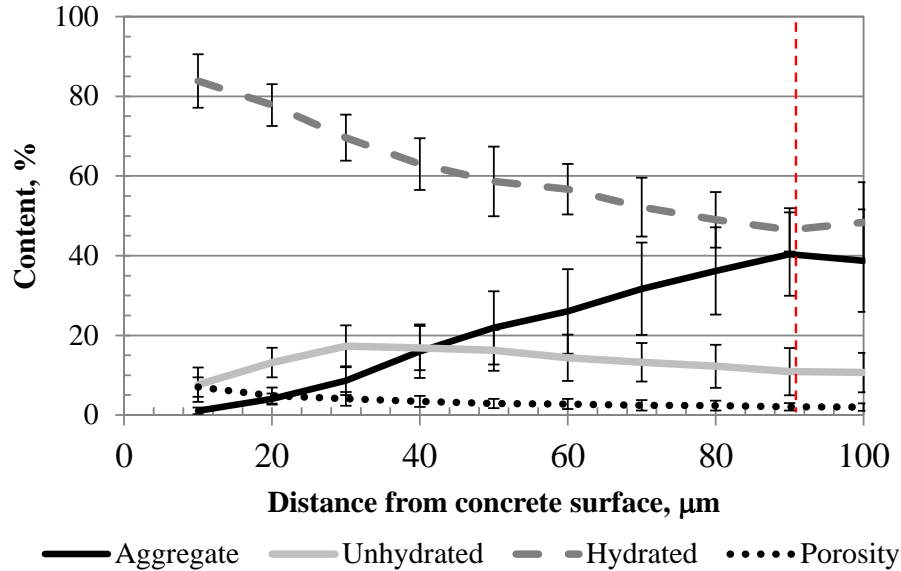


**Figure 36. Graph. Overall distribution at the interface as a function of distance from the concrete surface of specimen G2-8 phases.**

The content of unhydrated cement was below 8 percent in the 10- $\mu\text{m}$  gap close to the surface. The value reached a maximum of approximately 17 percent at 30  $\mu\text{m}$  away of the surface and progressively decreased to 10 percent at 100- $\mu\text{m}$  distance. The porosity also showed a maximum of 7 percent close to the interface in the 10- $\mu\text{m}$ -wide gap close to the surface. The high packing efficiency of the UHPC and low water-to-cement ratios explained the comparative low values of porosity relative to other overlay configurations where ordinary portland cement or grout materials were used. These systems typically showed porosity values on the interface on the order of from 30 to 20 percent. (De La Varga et al. 2017; Hans Beushausen, Höhlig, and Talotti 2017)

### TEST LOCATION G3

Specimens tested from region G3, which represented an apparent region of good bond without scarification prior to placement of the UHPC overlay, all failed in the concrete substrate (Mode 1). Peak stresses recorded prior to failure were between 344.6 psi (2.37 MPa) and 474.6 psi (3.27 MPa). Figure 37 shows a representative sample (G3-13) from the G3 test location. The bond between the UHPC overlay and the substrate concrete appears intact. Further, the difference in the UHPC-concrete interface texture can be observed when comparing the photos in Figure 31-C and Figure 37-C. Figure 38 shows the core location from which sample G3-13 was removed. As expected, apparent damage or delamination in the deck concrete or at the UHPC-concrete interface was not present.



A. Front of G3-13 specimen after testing.



B. Back of G3-13 specimen after testing.



C. UHPC-concrete interface of G3-13 specimen after testing.

**Figure 37. Photos. Specimen G3-13 after testing.**

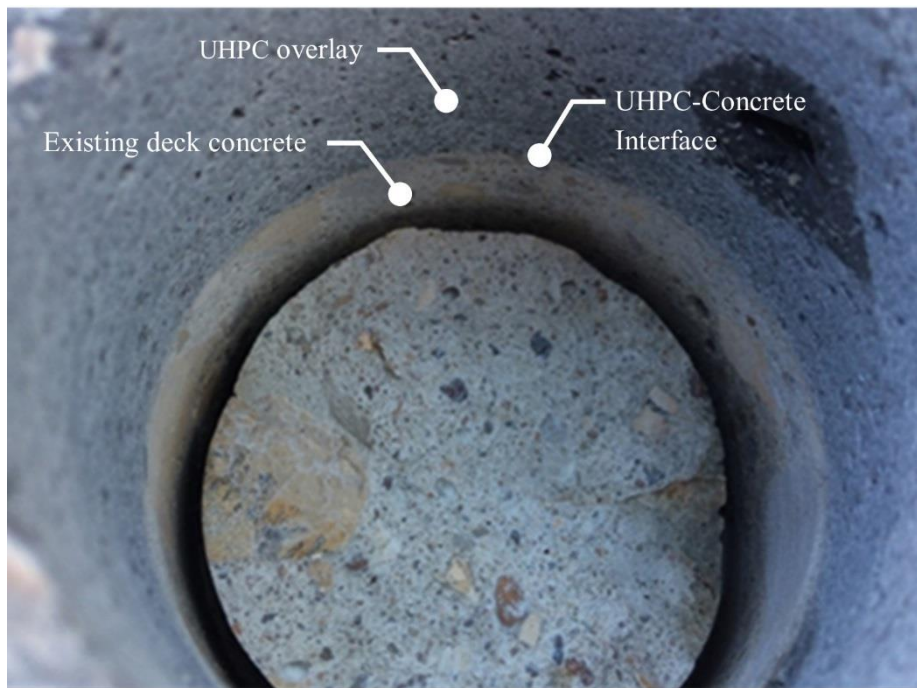


**Figure 38. Photo. Core location for specimen G3-13.**

The UHPC-concrete substrate interface of the G3-14 specimen had characteristics similar to those identified on the G2-8 sample. As shown in figure 39, the width of the UHPC paste adjacent to the concrete surface free of steel fibers varied between 0.024 in (0.6 mm) and 0.1 in (2.6 mm). This band was also characterized by its high degree of contact with the concrete surface. This was also motivated by high content of hydrated products of the UHPC paste in the vicinity of the concrete surface.

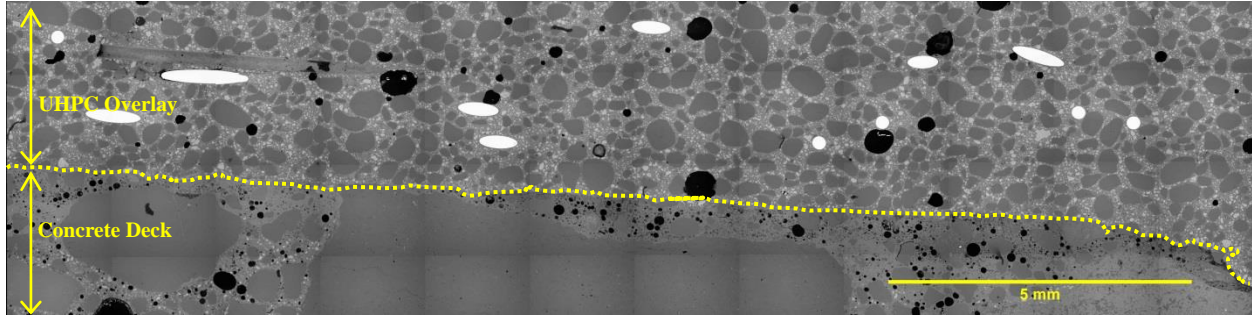


**Figure 39. Electron Microscope Image. General map of the UHPC-concrete interface for specimen G3-14.**

The main difference of this specimen relative to the two analyzed under the SEM is the absence of scarification on the concrete surface. This can be observed in the General map shown in figure 40, which shows that the interface line is relatively flat and lacks the “valley-hill” topography observed in the G2-8 sample shown in figure 33. This flat configuration contributed to improving the packing efficiency of the overlay material in direct contact with the substrate. (De La Varga et al. 2017) The direct consequence was a reduction in the wall effect on this interface compared with those having a valley-hill topography (surfaces previously subjected to scarification).

The trends in the distribution of phases on the interface for the G3-14 specimen, displayed in figure 40, were similar to those in the previous specimen, G2-8. Hydrated products of the UHPC paste were the principal phase in the first 100  $\mu\text{m}$  of the interface microstructure. Its value progressively decreased from 80 percent in the first 0 to 10  $\mu\text{m}$  to approximately 55 percent at 80  $\mu\text{m}$  away from the concrete surface. In parallel to the decrease in hydrated products, the aggregate content increased from 0 percent right at the interface to a value of approximately 25 percent at 80  $\mu\text{m}$ . The content of both unhydrated particles and porosity evolved following the same trend as the one observed in specimen G2-8. In the case of the unhydrated particles, the initial 8 percent content right at the surface increased to approximately 20 percent at 30  $\mu\text{m}$  away of the surface and progressively decreased to 10 percent at 100- $\mu\text{m}$  distance. While at initial 10 percent value of porosity, the interface constantly diminished to below 2 percent at 100- $\mu\text{m}$  distance from the surface.

Finally, the distribution graph in figure 40 also confirms a reduction in the extent of the UHPC paste affected by the wall effect induced by the “plateau” configuration of the concrete surface. The inflexion point in this G3-14 specimen was observed at 80- $\mu\text{m}$  distance from the surface instead of the 90- $\mu\text{m}$  mark registered in the previous specimen (G2-8).

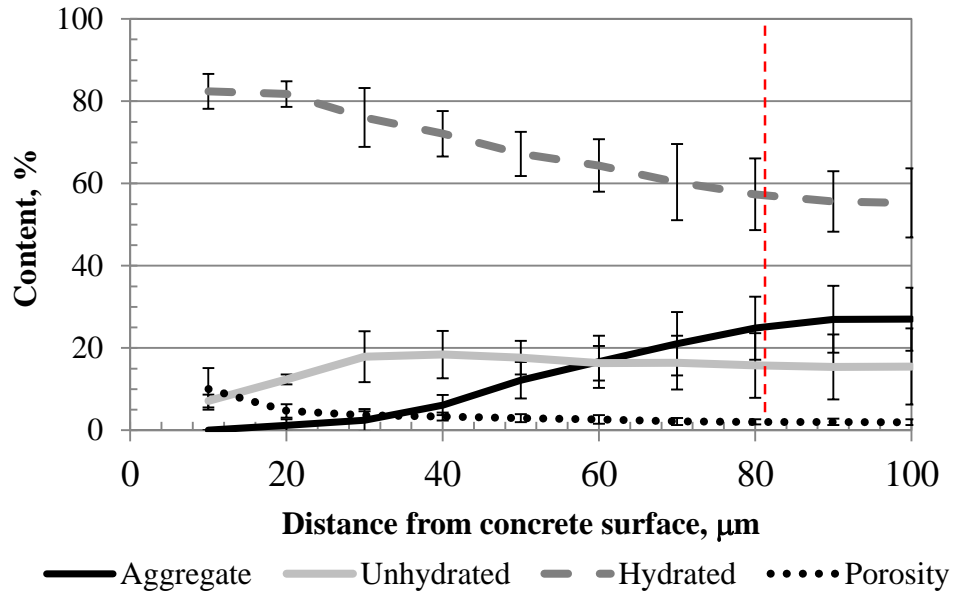


**Figure 40. Graph. Overall distribution at the interface as a function of distance from the concrete surface of specimen G3-14 phases.**

#### TEST LOCATIONS B1 AND B7

Specimens tested from regions B1 and B7, which represented regions of potential delamination with scarification prior to placement of the UHPC overlay, all failed in the concrete substrate (Mode 1). Peak stresses recorded prior to failure were between 0 psi (0 MPa) and 114 psi (0.79 MPa), which were relatively low compared with other regions. Two of the four samples (B1-3 and B7-12) were loose after completing the coring procedure. These two samples were removed without applying load (i.e., they were loose after completing the particle coring). Further examination of the four test samples and their respective core locations indicated that pre-existing delamination was present in the conventional concrete deck. Figure 41 shows a representative sample (B7-11) from the B1 and B7 test locations. Although the bond between the UHPC overlay and the substrate concrete appears intact, pre-existing damage can be observed within the concrete substrate layer.

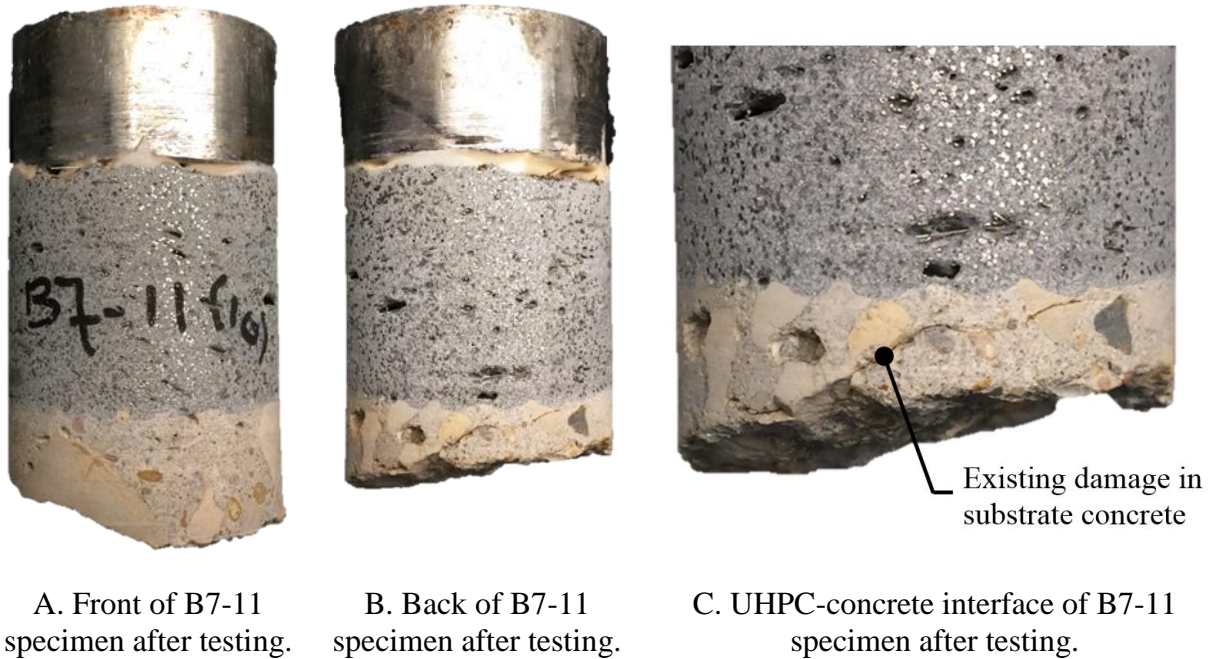


**Figure 41. Photos. Specimen B7-11 after testing.**

This can be most clearly observed in figure 42, which shows the core location from which sample B7-11 was removed. A horizontal crack plane can be observed within the concrete deck layer approximately 0.5 in (12 mm) below the UHPC-concrete interface. Further, it is evident that when sample B7-11 failed, failure was initiated from this existing crack plane.

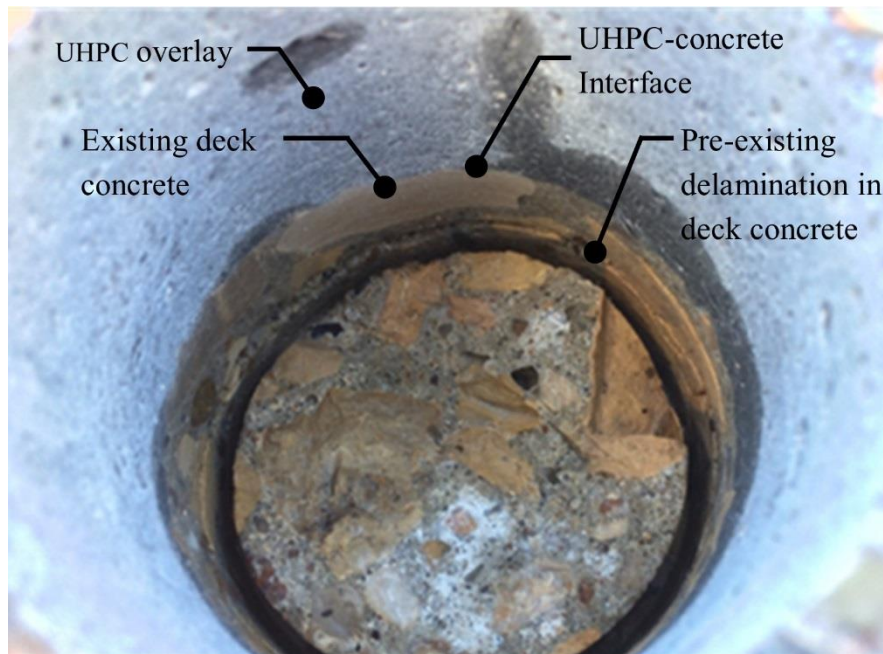


**Figure 42. Photo. Core location for specimen B7-11.**

The microstructural analysis of specimen B7-12 also revealed a dense interface dominated by the presence of hydrated products, as in the previous two samples. In this case, the width of the UHPC band without steel fibers ranged from 0.024 in (0.6 mm) to 0.12 in (3.0 mm). The typical valley-hill topography was observed on the concrete surface as illustrated in figure 43. Additionally, as in the case of the G2-8 specimen, entrapped air and accumulated debris were visualized disrupting the contact between UHPC hydrated products and concrete surface. However, the extent of this disruption was limited, and it was not expected to have a deleterious effect on the overall bond strength of the system.

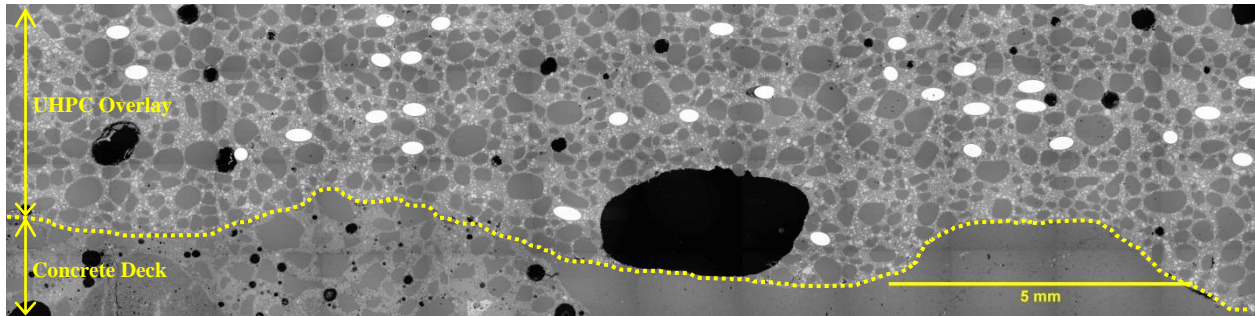


**Figure 43. Electron Microscope Image. General map of the UHPC-concrete interface for specimen B7-12.**

As shown in figure 44, the results of quantitative analysis for this specimen are similar to those measured in G2-8. At the interface, the hydrated products were above 80 percent, and porosity was around 7 percent. The aggregate content showed a similar evolution, reaching 40 percent at 100- $\mu\text{m}$  distance from the interface. This similarity with the G2-8 specimens also extended to the distance where the inflexion point in the trend of hydrated particles and aggregate was located. Based on the data shown in figure 44, it was inferred that this limit was located close to 100- $\mu\text{m}$  distance from the surface. Significantly, this sample came from a location where the concrete surface was subjected to scarification. Thus, as in specimen G2-8, the distance from where the inflexion point occurred was significantly higher than the distance observed for the nonscarified sample (G3-12).

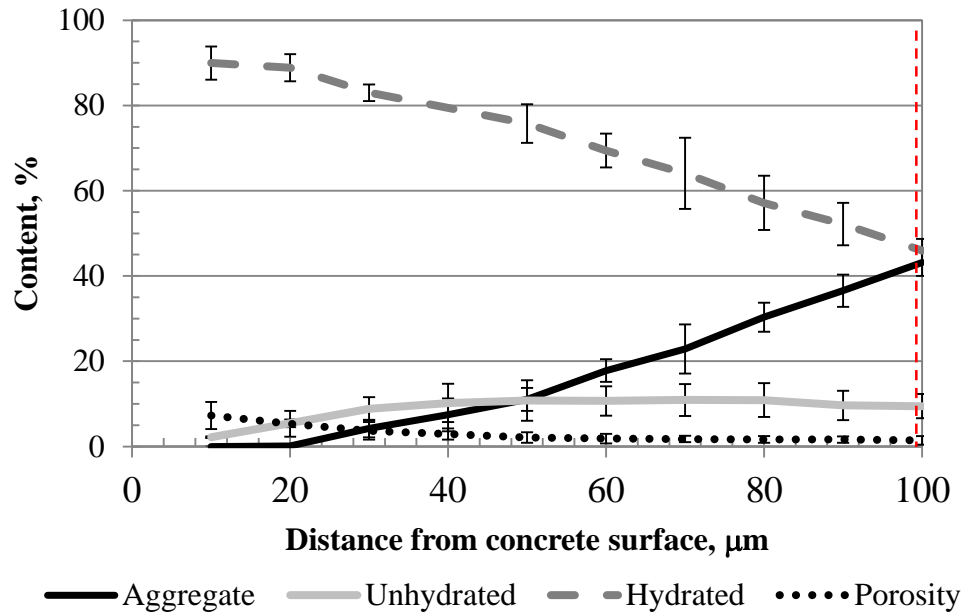


**Figure 44. Graph. Overall distribution at the interface as a function of distance from the concrete surface of the specimen B7-12 phases.**

## SUMMARY OF RESULTS

Generally speaking, results indicated good bonding between the UHPC overlay and the substrate concrete deck, with and without scarification prior to overlay placement. Peak tensile stresses sustained by specimens in regions G1, G2, and G3 prior to failure were comparable if not higher than the bond strengths of other UHPC-class materials (nonthixotropic) bonded to a roughened concrete substrate. (Haber and Graybeal 2016)

Furthermore, peak tensile stresses sustained by these specimens were, in most cases, higher than those exhibited by conventional grout-like materials bonded to a roughened concrete substrate. (De La Varga, Haber, and Graybeal 2017)

As for regions of potential delamination, it was found that bond between the UHPC overlay and the substrate concrete was intact, based on visual inspection. The UHPC-concrete interface appeared similar to that observed in samples taken from locations G1, G2, and G3. It was evident that failure of specimens from regions B1 and B7 was the result of pre-existing concrete deck delamination. This caused specimens to carry little-to-no tensile load prior to failure. Notably, other regions of potential delamination (B2, B6, and B8) were not tested, and findings from tests completed at locations B1 and B7 may not extrapolate to these locations. Many of these untested regions were small and located near the boundaries of the two overlay stages.

## CHAPTER 6. SUMMARY AND CONCLUSIONS

The first U.S. deployment of UHPC as a bridge deck overlay was completed in May 2016 on a reinforced concrete slab bridge located in Brandon, IA, in Buchanan County. A few months after installing the UHPC overlay, a field inspection of the bridge concluded that there could be some potential locations of deck delamination. However, it was not known whether delamination, if actually present, occurred at the interface between the UHPC overlay and substrate concrete, within the existing concrete deck, or within the UHPC overlay itself. The bond between the UHPC overlay and substrate concrete needed assessment. In November 2016, researchers from FHWA's TFHRC conducted a field study to evaluate the bond between the UHPC overlay and the substrate concrete bridge deck.

Based on observations and data collected, it can be concluded that the bond between the UHPC overlay and the existing concrete bridge deck was intact. Mechanical testing verified that the locations suspected of having good UHPC-concrete bond were able to carry relatively high tensile stresses without bond failure. It can also be concluded that good bond was achieved even at locations where deck concrete was not roughened (scarified) prior to placement of the UHPC overlay; however, this was dependent on the surface quality of the substrate concrete and is not a recommended practice. The two test locations suspected of delamination were indeed found to have delaminated concrete. However, delamination was pre-existing within the deck concrete and was likely present prior to placement of the UHPC overlay.

In all cases, visual inspection of the UHPC-concrete interface indicated that the interface between the UHPC overlay and deck concrete appeared intact. This was further investigated through microstructural analysis using a scanning electron microscope. Microstructural analysis revealed a high density of UHPC in direct contact with the concrete substrate surface in all cases studied. This high density was caused by the high content of hydration products from the UHPC and low porosity adjacent to the interface. The consequence of this was a high degree of direct contact between the UHPC and the concrete surface, which translated into high tensile strength of the interface.

Microstructural analysis also revealed an absence of steel fibers near the UHPC-concrete interface in all cases studied. That is, no steel fibers were observed on the UHPC paste band in direct contact with the concrete surface. Thus, fibers did not contribute directly to adhesion of the paste to the surface of concrete.

Comparison of phase distribution evolution at the interface revealed no significant difference in the trends of porosity, aggregate, and hydrated/unhydrated particles at the studied micro-scale between scarified and nonscarified concrete surface. However, two small differences were observed between scarified and nonscarified concrete: (1) features disrupting the contact between UHPC and concrete such as air void and accumulated debris were found on the interface of the two specimens where the concrete was scarified; and (2) the extent of the wall effect was higher in those UHPC overlays placed on top of a scarified concrete surface in comparison to those placed over a nonscarified surface. Neither of these observed differences had any effect on the tensile strength of the interface bond.



## REFERENCES

- Aaleti, Sriram, S. Sritharan, and A. Abu-Hawash. 2013. "Innovative UHPC-Normal Concrete Composite Bridge Deck." RILEM-fib-AFGC International Symposium on Ultra-High Performance Fibre-Reinforced Concrete.
- American Society of Testing and Materials. (ASTM) C1437-15. 2015. *Standard Test Method for Flow of Hydraulic Cement Mortar*. West Conshohocken, PA: ASTM International.
- . C1583/C1583M-13. 2013. *Standard Test Method for Tensile Strength of Concrete Surfaces and the Bond Strength or Tensile Strength of Concrete Repair and Overlay Materials by Direct Tension (Pull-off Method)*. West Conshohocken, PA: ASTM International.
- Beushausen, H., and M. Gillmer. 2014. "The Use of Superabsorbent Polymers to Reduce Cracking of Bonded Mortar Overlays." *Cement and Concrete Composites*, 52:1–8.
- Beushausen, H., B. Höhlig, and M. Talotti. 2017. "The Influence of Substrate Moisture Preparation on Bond Strength of Concrete Overlays and the Microstructure of the OTZ." *Cement and Concrete Research*, 92:84–91.
- Beyene, M., J. F. Munoz, R. Meininger, and C. Di Bella. 2016. "Effect of Internal Curing as Mitigation to Minimize ASR Damage." *ACI Materials Journal*, 114;3:417-428.
- Brühwiler, E., and E. Denarié. 2013. "Rehabilitation and Strengthening of Concrete Structures Using Ultra-High Performance Fibre Reinforced Concrete." *Structural Engineering International*, 23;4:450–457.
- Brühwiler, E., M. Bastien-Masse, H. Mühlberg, B. Houriet, B. Fleury, S. Cuennet, P. Schär, F. Boudry, and M. Maurer. 2015. Strengthening the Chillon viaducts deck slabs with reinforced UHPFRC. Proceedings, 2015 IABSE Conference, Geneva, Switzerland.
- De La Varga, I., Z. B. Haber, and B. Graybeal. 2017. "Bond of Field-Cast Grouts to Precast Concrete Elements." *FHWA-HRT-16-081*. Washington, DC: Federal Highway Administration.
- Diamond, S., and J. Huang. 2001. "The ITZ in Concrete - a Different View Based on Image Analysis and SEM Observations." *Cement and Concrete Composites*, 23;2-3:179–188.
- El Sharief, A., M. D. Cohen, and J. Olek. 2003. "Influence of Aggregate Size, Water Cement Ratio and Age on the Microstructure of the Interfacial Transition Zone." *Cement and Concrete Research*, 33;11:1837–1849.
- El-Tawil, S., M. Alkaysi, A. E. Naaman, W. Hansen, and Z. Liu. 2016. "Development, Characterization and Applications of a NonProprietary Ultra High Performance Concrete for Highway Bridges." RC-1637. University of Michigan.
- Garboczi, E. J., and D. P. Bentz. 1991. "Digital Simulation of the Aggregate–cement Paste Interfacial Zone in Concrete." *Journal of Materials Research*, 6;1:196–201.
- Graybeal, B. A. 2006. "Material Property Characterization of Ultra-High Performance Concrete." *FHWA-HRT-06-103*. Washington, DC: Federal Highway Administration.
- . 2011. "Ultra-High Performance Concrete." *FHWA-HRT-11-038*. Washington, DC: Federal Highway Administration.

- Graybeal, B. A., and F. Baby. 2013. "Development of Direct Tension Test Method for Ultra-High- Performance Fiber-Reinforced Concrete." *ACI Materials Journal*, 110;2:177–86.
- Graybeal, B. A., and B. Stone. 2012. "Compression Response of a Rapid-Strengthening Ultra-High Performance Concrete Formulation." *FHWA-HRT-12-065*. Washington, DC: Federal Highway Administration.
- Habel, K., E. Denarié, and E. Brühwiler. 2007. "Experimental Investigation of Composite Ultra-High-Performance Fiber-Reinforced Concrete and Conventional Concrete Members." *ACI Structural Journal*, 104;1:93–101.
- Haber, Z., and B. A. Graybeal. 2016. "Performance of Different UHPC-Class Materials in Prefabricated Bridge Deck Connections." Proceedings, First International Interactive Symposium on UHPC, Des Moines, IA, July 18–20, 2016.
- Krauss, P. D., J. S. Lawler, and K. A. Steiner. 2009. "Guidelines for Selection of Bridge Deck Overlays, Sealers, and Treatments." *NCHRP Project Report 20-07*.
- Noshiravani, T., and E. Bruhwiler. 2013. "Experimental Investigation on Reinforced Ultra-High-Performance Fiber-Reinforced Concrete Composite Beams Subjected to Combined Bending and Shear." *ACI Materials Journal*, 110;2:251–261.
- Ollivier, J.P., J.C. Maso, and B. Bourdette. 1995. "Interfacial Transition Zone in Concrete." *Advanced Cement Based Materials*, 2;1:30–38.
- Sajna, A., E. Denarié, and V. Bras. 2012. "Assessment of a UHPFRC Based Bridge Rehabilitation in Slovenia, Two Years after Application." Proceedings, 3rd International Symposium on Ultra-High Performance Concrete. HiPerMat, Marseille, France.
- Scrivener, K. L., A. K. Crumbie, and P. Laugesen. 2004. "The Interfacial Transition Zone (ITZ) Between Cement Paste and Aggregate in Concrete." *Interface Science*, 12;4:411–421.
- Shann, S. V. 2012. Application of Ultra High Performance Concrete (UHPC) as a Thin-Bonded Overlay for Concrete Bridge Decks. M.S. Thesis, Michigan Technological University
- Swenty, M. K., and B. A. Graybeal. 2013. "Material Characterization of Field-Cast Connection Grouts." *NTIS No. PB2013-130231*. Washington, DC: Federal Highway Administration.
- Toutlemonde, F., P. Marchand, F. Gomes, and L. Dieng. 2013. "Using UHPFRC as a Topping Layer for Orthotropic Bridge Decks: Prototype Validation." Proceedings, 3rd International Symposium on Ultra-High Performance Concrete, HiPerMat, Marseille, France.
- Wille, K., and C. Boisvert-Cotulio. 2013. "Development of Non-Proprietary Ultra-High Performance Concrete for Use in the Highway Bridge Sector." *FHWA-HRT-13-100*. Washington, DC: Federal Highway Administration.



